

**BULLETIN N° 210**  
**ACADÉMIE EUROPEENNE**  
**INTERDISCIPLINAIRE**  
**DES SCIENCES**  
**INTERDISCIPLINARY EUROPEAN ACADEMY OF SCIENCES**



**Lundi 5 décembre 2016 :**  
**à 17 h à la Maison de l'AX, 5 rue Descartes 75005 PARIS**

**Conférence de Zsolt LENKEI**  
**Directeur de Recherche à l'INSERM**  
**Laboratoire de Plasticité du Cerveau ESPCI-CNRS**  
**" Rôle de la contraction de l'actomyosine par les cannabinoïdes dans la structure et la connectivité neuronale à de multiples échelles spatio-temporelles "**

**Notre Prochaine séance aura lieu le lundi 9 janvier 2017 à 17h**  
**5 rue Descartes 75005 PARIS**  
 Elle aura pour thème

**Conférence du Dr Stein SILVA**  
**MCU / PH Service de Réanimation / INSERM U825**  
**CHU Purpan / Toulouse**  
**" Apparition de la conscience à partir du coma: état de la science "**

# ACADÉMIE EUROPÉENNE INTERDISCIPLINAIRE DES SCIENCES INTERDISCIPLINARY EUROPEAN ACADEMY OF SCIENCES

**PRÉSIDENT** : Pr Victor MASTRANGELO  
**VICE PRÉSIDENT** : Pr Jean-Pierre FRANÇOISE  
**VICE PRÉSIDENT BELGIQUE**(Liège):  
 Pr Jean SCHMETS  
**VICE PRÉSIDENT ITALIE**(Rome):  
 Pr Ernesto DI MAURO  
**SECRÉTAIRE GÉNÉRALE** : Irène HERPE-LITWIN  
**SECRETARIAIRE GÉNÉRALE Adjointe** : Marie-Françoise  
 PASSINI  
**TRÉSORIÈRE GÉNÉRALE**: Édith PERRIER

**MEMBRES CONSULTATIFS DU CA** :  
 Gilbert BELAUBRE  
 François BÉGON  
 Bruno BLONDEL  
 Michel GONDRAN

**COMMISSION FINANCES**: Claude ELBAZ  
**COMMISSION MULTIMÉDIA**: Pr. Alain CORDIER  
**COMMISSION SYNTHÈSES SCIENTIFIQUES**:  
 Jean-Pierre TREUIL  
**COMMISSION CANDIDATURES**:  
 Pr. Jean-Pierre FRANÇOISE

**PRÉSIDENT FONDATEUR** : Dr. Lucien LÉVY (†)  
**PRÉSIDENT D'HONNEUR** : Gilbert BELAUBRE

**CONSEILLERS SCIENTIFIQUES** :  
**SCIENCES DE LA MATIÈRE** : Pr. Gilles COHEN-TANNOUDI  
**SCIENCES DE LA VIE ET BIOTECHNIQUES** : Pr Ernesto DI MAURO

**CONSEILLERS SPÉCIAUX**:  
**ÉDITION**: Pr Robert FRANCK  
**AFFAIRES EUROPÉENNES** :Pr Jean SCHMETS  
**RELATIONS VILLE DE PARIS et IDF**:  
 Michel GONDRAN ex-Président/ Claude MAURY  
**MOYENS MULTIMÉDIA et RELATIONS UNIVERSITÉS**:  
 Pr Alain CORDIER  
**RELATIONS AX**: Gilbert BELAUBRE  
**MECENAT**: Pr Jean Félix DURASTANTI  
**GRANDS ORGANISMES DE RECHERCHE NATIONAUX ET  
 INTERNATIONAUX**: Pr Michel SPIRO

**SECTION DE NANCY** :  
**PRESIDENT** : Pr Pierre NABET

décembre 2016

**N°210**

TABLE DES MATIERES

p. 03 Séance du 5 décembre 2016 :  
 p. 06 Annonces  
 p. 07 Documents

**Prochaine séance : lundi 9 janvier 2017**

**Conférence du Dr Stein SILVA  
 MCU / PH Service de Réanimation / INSERM U825  
 CHU Purpan / Toulouse  
 " Apparition de la conscience à partir du coma: état de la science"**

**ACADEMIE EUROPEENNE INTERDISCIPLINAIRE DES SCIENCES**  
**INTERDISCIPLINARY EUROPEAN ACADEMY OF SCIENCES**

5 rue Descartes 75005 PARIS

**Séance du Lundi 5 décembre 2016 /Maison de l'AX 17h**

La séance est ouverte à 17h **sous la Présidence de Victor MASTRANGELO** et en la présence de nos Collègues Gilbert BELAUBRE, Jean-Louis BOBIN, Alain CARDON, Jean-Felix DURASTANTI, Françoise DUTHEIL, Claude ELBAZ, Michel GONDRAN, Irène HERPE-LITWIN, Claude MAURY, PASSINI Marie-France, Jacques PRINTZ, Jean SCHMETS , Jean-Pierre TREUIL .

Etaient excusés :François BEGON, Jean-Pierre BESSIS, Bruno BLONDEL, Michel CABANAC, Juan-Carlos CHACHQUES, Gilles COHEN-TANNOUDJI, Alain CORDIER , Daniel COURGEAU, Ernesto DI MAURO, Vincent FLEURY, Robert FRANCK, Jean -Pierre FRANCOISE, Jacques HENRI-ROBERT, Dominique LAMBERT, Gérard LEVY, Valérie LEFEVRE-SEGUIN, Antoine LONG, Pierre MARCHAIS, Anastassios METAXAS, Jacques NIO, Edith PERRIER, Pierre PESQUIES, Michel SPIRO, Alain STAHL, Jean VERDETTI.

**I. Présentation de notre conférencier Zsolt LENKEI par notre Président Victor MASTRANGELO**

Voici le CV résumé de notre conférencier:

**CV Zsolt LENKEI**

- Nom: LENKEI
- Prénom: Zsolt
- Né le 11 février 1967 à Budapest, Hongrie
- Nationalité: Hongroise
- **Parcours Universitaire :**
  - 1991: Doctorat en Médecine Faculté de médecine de l'Université Semmelweis de Budapest
  - 1998: PhD en neurosciences Université Pierre et Marie Curie (Paris 6)
  - 2009: Habilitation à Diriger des Recherches (HDR) en neurosciences Université Pierre et Marie Curie (Paris 6)
- **Postes actuels:**
  - Directeur de Recherche (DR2) à l'INSERM au Laboratoire de plasticité du Cerveau ESPCI-CNRS UMR 8249, ESPCI Paris
  - Nommé en tant que chef d'équipe senior ( à partir de 2017) du nouveau Centre "Psychiatrie et Neurosciences" de Paris
- **Postes occupés précédemment**
  - 1993-1998: Etudiant doctorant dans l'Unité U 36 de l'INSERM, Collège de France, Paris
  - 1998: Chercheur post-doctorant dans le service du Pr Alain BEAUDET de l'Université Mc Guill de Montréal , Canada
  - 1998-2000: Titularisation en tant que chercheur à l'INSERM, Unité INSERM U 36, Collège de France Paris
  - 2000: Titularisation en tant que Chercheur à l'INSERM à l'ESPCI-CNRS UMR 7637 devenue UMR 8249 ESPCI de Paris

- **Enseignement**

- 2001-2008 : Préceptorat en Biologie , ESPCI-Paris Tech, niveau M -Paris
- 2010-2017 : Préceptorat en Physiologie , ESPCI-Paris Tech, niveau M Paris
- 2015-2017 : Professeur de Biologie, à l'Université de Recherche Paris-Sciences- Lettres (PSL) niveau L2, 48heures par an

- **Affiliation Ecoles doctorales:**

- 
- Cerveau-Cognition - Comportement (ED3C, ED n°158)

- **Appartenance à des sociétés savantes:**

- Société des Neurosciences
- American Neuroscience Society

- **Nominations et distinctions scientifiques**

- 1996: Médaille de jeune chercheur de la Société de Neuroendocrinologie Servier
- 2008: Conférence Plénière Jancso, IBRO Conférence Internationale sur les Réseaux neuronaux complexes de Debrecen /Hongrie
- 2014: Prix Jean Langlois
- 2015: Elu co-président de pour la conférence de 2017 Gordon Research Conference on Cannabinoid Function in the CNS', dans le New Hampshire USA

- **Langues:**

- Français, anglais, allemand , hongrois

- **Invitations en tant que conférencier dans des événements scientifiques internationaux :**

- Gordon Conference on Cannabinoid Function in the CNS, 2005, Lewiston, ME
- 7th. Melbourne GPCR Forum, 2005, Howard Florey Institute, Melbourne, Australia
- ASCEPT Annual Scientific Meeting (Australasian Society of Clinical and Experimental Pharmacologists and Toxicologists, 2005, Melbourne, Australia
- Gordon Conference on Cannabinoid Function in the CNS, 2007 Les Diablerets, Suisse)
- Jancso Plenary Lecture at the IBRO International Workshop on Complex Neuronal Networks, 2007, Debrecen, Hungary
- Meeting of the Federation of European Neuroscience Societies (FENS), 2008, Geneva, Switzerland
- 3rd Course on Cytoskeleton, 2011, Curie Institut, Paris, France
- Workshop "Physique des Ondes pour la Médecine", 2014, Crète, Grèce,
- Congrès du GDR-3545 (groupe de Recherche CNRS sur les GPCR), 2014, Montpellier
- Mainz University, 2014; Mainz, Germany,
- Gordon Conference on Cannabinoid Function in the CNS, 2015, Lucca (Barga), Italy
- Cannabinoid Conférence 2015, Sestri-Levante, Italy
- Instructor at the IBRO-Kemali Workshop, 2015, Naples, Italy
- Institut of Experimental Medecine, Hungarian Academy of Sciences, 2015, Budapest, Hungary
- Munich-TUM mini-symposium, Technical University of Munich, 2015, Munich, Germany
- Selected talk at the Conférence Jacques Monod "Optical imaging of brain connectivity" 2016, Roscoff (Brittany), France
- 8th Course on Cytoskeleton, 2016, Curie Institut, Paris, France
- Course "Principles and Applications of Fluorescence Microscopy", 2017, Pasteur Institut, Paris,

France

- **Obtention Financements**

- 2010-2012: ANR-09-MNPS-004-01, **480 000€** *Coordinateur Zsolt Lenkei, collaborateurs: INSERM U894, Centre Psychiatrie et Neurosciences (Therese Jay), Institut Langevin ESPCI-ParisTech (Ralph Sinkus, Mickael Tanter)*
- 2013-2014: Défi Innovations Thérapeutiques pour les Maladies Mentales (ITMM), **30 000€** *Coordinatrice Laurence Lafarechene, Institut Albert Bonniot, CRI INSERM/UJF U823, Grenoble*
- 2015-2017: Université de Recherche PSL, projet MyoSynapse, 3 équipes, coordinateur Z. Lenkei, **150 000€-**
- (**83 000€**pour l'équipe)
- 2016-2018: FUSIMICE, FLAG-ERA Joint Transnational Call 2015, *Human Brain Project*, 4 équipes,
- *coordinateur Z. Lenkei, 780 000€(233 000€for the team)*
- 2016-2018: Université de Recherche PSL - projet NanoPaint, 2 équipes, coordinatrice Diana Zala (équipe Z Lenkei) **69 000€**

- **Publications:**

- Web of Science at 2016 October: N° of publications: **56**, N° of citations (without self-citations): **1714 (1633)**, h-index: **21**

- **Une sélection de 15 publications dans des revues à comité de lecture:**

Notre conférencier a fait acte de candidature en tant que membre titulaire de l'AEIS. Sa candidature sera très prochainement examinée.

## II. Conférence de Zsolt LENKEI

Résumé en français de la présentation de Zsolt LENKEI:

### **Rôle de la contraction de l'actomyosine induite par les cannabinoïdes dans la structure et la connectivité neuronale à de multiples échelles spatio-temporelles**

Nous avons récemment montré l'induction d'un remodelage rapide par les cannabinoïdes du cytosquelette neuronal constitué d'actomyosine avec des conséquences potentiellement importantes sur le développement du câblage du cerveau. Nos résultats récents mettent en évidence un rôle de la contraction de l'actomyosine induite par les cannabinoïdes dans la plasticité synaptique. En complément de nos outils *in vitro* et *ex vivo*, nous participons au développement interdisciplinaire d'un nouveau mode d'imagerie *in vivo* utilisant des Ultrasons fonctionnels cérébraux rapides ( *en anglais: functional fast brain ultrasound (fUS)* ) pour explorer le rôle de la contraction de l'actomyosine induite par les cannabinoïdes au niveau de la structure et de la connectivité du cerveau d'un rongeur vivant. Les *fUS* fournissent une imagerie comparable à celle des IRM fonctionnels (*fMRI*) pour des animaux anesthésiés et en état d'éveil, avec des gains de résolution de plusieurs ordres de grandeur par rapport à ceux des *fMRI*.

Un compte-rendu détaillé sera prochainement disponible sur le site de l'AEIS, <http://www.science-inter.com>

# Annonces

- I. **Quelques ouvrages papiers relatifs au colloque de 2014 " Systèmes stellaires et planétaires- Conditions d'apparition de la Vie" -**
- Prix de l'ouvrage :25€.
  - Pour toute commande s'adresser à :

Irène HERPE-LITWIN Secrétaire générale AEIS  
39 rue Michel Ange 75016 PARIS  
06 07 73 69 75  
[irene.herpe@science-inter.com](mailto:irene.herpe@science-inter.com)

## Documents

Pour préparer sa conférence Stein SILVA nous a communiqué:

- p.08: un résumé de sa conférence en anglais traduit en français
- p.09: un article paru dans "le Monde " du 11/11/2015 " Prédire la sortie du coma grâce à l'imagerie Cérébrale"
- p. 11: un article signé par Stein SILVA et coll intitulé "Disruption of posteromedial large-scale neural communication predicts recovery from coma" publié dans Neurology® 2015;85:1–9

Pour compléter la conférence du Dr Zsolt LENKEI nous vous proposons ,

- p. 21 issu de Front. Cell. Neurosci., 06 January 2015 | <https://doi.org/10.3389/fncel.2014.00426> , un article intitulé " *Polarized cellular patterns of endocannabinoid production and detection shape cannabinoid signaling in neurons*" cosigné par Zsolt LENKEI .

Séance du lundi 9 janvier 2017

Dr. Stein SILVA (MD, PhD)  
Reanimation / Critical Care Unit  
INSERM U825  
CHU Purpan / Purpan University Teaching Hospital  
31059 Toulouse Cedex 3, FRANCE

**Abstract:**

**Consciousness emergence from coma: the state of the science.**

The concept of consciousness continues to defy definition and elude the grasp of philosophical and scientific effort to formulate a testable framework for conscious experience. Severe acquired brain injury results in the dissolution of consciousness providing a lesional model from which key insights about the emergence of human consciousness may be drawn. In the clinical setting, specialist faces the challenge of detecting and monitor consciousness recovery, in brain-injured patients who are initially unable to communicate through word or gesture.

Findings from neuroimaging and electrophysiology have garnered scientific and clinical attention in light of increased evidence that they can detect active cognitive processing, and identify the structural and functional brain architecture changes that are related to pathological loss of consciousness. We will provide an overview that describe the state of the science of this research, with regard to potential clinical implication for the management of comatose patients and the bioethical issues that are unique to this population.

**Résumé**

**Apparition de la conscience à partir du coma: état de la science**

Le concept de conscience continue à braver toute définition et à échapper à l'effort philosophique et scientifique de formulation d'un schéma testable de l'expérience consciente. Subir une blessure cérébrale sévère crée une perte de conscience ce qui fournit un modèle de lésion à partir duquel on peut trouver des idées-clé concernant l'apparition de la conscience. En milieu clinique le spécialiste est confronté au défi de détection et de suivi de récupération de la conscience chez des patients ayant subi une blessure du cerveau qui sont dans un premier temps dans l'incapacité de communiquer verbalement ou gestuellement.

Les découvertes en neuro-imagerie et en électrophysiologie ont suscité l'attention des scientifiques et des cliniciens car de plus en plus d'éléments tendent à montrer qu'ils peuvent détecter des processus actifs de cognition et identifier les changements structurels et fonctionnels du cerveau en relation avec une perte de conscience pathologique. Nous allons fournir un aperçu de l'état de la science dans ce domaine en s'intéressant particulièrement aux retombées cliniques potentielles dans le domaine du traitement des patients comateux et aux problèmes éthiques propres à cette population.

## Prédire la sortie du coma avec l'imagerie cérébrale (Le Monde 11/11/2015)

**Selon des travaux de l'Inserm, le pronostic est lié à la qualité de la connexion entre deux zones du cerveau**

Va-t-il sortir du coma ? A cette question qui taraude les familles, les travaux d'une équipe de l'Institut national de la santé et de la recherche médicale (Inserm) apportent un nouvel élément de réponse. En étudiant, par imagerie à résonance magnétique (IRM) fonctionnelle, le cerveau d'une trentaine de patients plongés dans le coma à la suite d'un traumatisme crânien ou d'un arrêt cardiaque, comparativement à celui d'individus sans trouble neurologique, Stein Silva, réanimateur au CHU de Toulouse, et ses collègues montrent que le degré de communication entre deux zones cérébrales permet de prédire quels individus vont récupérer leur conscience dans les mois suivant l'accident. Ces travaux novateurs sont publiés dans la revue *Neurology*, datée du mercredi 11 novembre.

Altération plus ou moins sévère de la conscience de soi-même et de l'environnement, le coma -concerne chaque année des dizaines de milliers de personnes en France. Il peut résulter de nombreuses causes, dont les plus fréquentes sont l'hypoxie (manque d'oxygénation) cérébrale après un arrêt cardiaque, un traumatisme crânien ou un accident vasculaire cérébral, en particulier par hémorragie. Cet état transitoire dure au maximum quelques semaines. Le devenir des patients est très -variable. Certains meurent. D'autres, au contraire, se réveillent en quelques jours. La récupération peut être beaucoup plus lente et passer par des états de conscience altérée : état végétatif et état de conscience minimal.

L'état végétatif correspond à des patients qui ont des cycles de veille et de sommeil (avec ouverture spontanée des yeux), mais aucun signe de conscience. Leurs seuls mouvements sont réflexes. L'état de conscience minimale est, lui, défini par la présence – parfois fugace mais reproductible – de signes de conscience : -verbalisation, poursuite visuelle...

Dans le monde, des équipes très spécialisées explorent ces états de conscience altérée et les comas, pour essayer d'affiner au mieux le diagnostic et le pronostic. La prédiction de l'avenir de ces malades reste cependant souvent difficile.

### Perspectives thérapeutiques

Ces recherches, qui font appel à de nombreuses techniques (imagerie cérébrale, étude de l'activité électrique du cerveau...), permettent aussi d'élucider peu à peu les mécanismes de la conscience à l'échelle neuronale. Ainsi, on sait désormais qu'il n'y a pas un siège unique de la conscience, mais qu'il s'agit d'un " espace de travail -global ", une sorte de conversation entre différentes parties du cerveau.

L'équipe de Stein Silva et Patrice Péran (spécialiste en neuro-imagerie) a comparé l'activité cérébrale de 27 personnes dans le coma (14 à la suite d'un traumatisme crânien et 13 après un arrêt cardiaque) et de sujets du même âge sans trouble neurologique, grâce à une IRM fonctionnelle. Les chercheurs se sont particulièrement intéressés à une zone postérieure du cerveau, le cortex postéro-médian (CPM). Cette région est en effet impliquée dans d'autres formes de perte de conscience : son activité est, par exemple, abaissée pendant le sommeil ou lors d'une anesthésie.

Chez tous les patients dans le coma, quelle qu'en soit l'origine, Stein Silva et ses collègues ont observé une " *perte de communication majeure* " entre le CPM et la partie antérieure du cerveau (cortex frontal médian). Une observation qui, selon eux, suggère le rôle important de l'interaction entre ces deux structures dans l'émergence de la conscience humaine.

De plus, ils ont étudié le niveau d'altération de cette connexion au cours du temps et montré qu'il était corrélé à l'état neurologique du patient trois mois plus tard. " *Les malades qui vont récupérer un état de conscience présentent des niveaux de connexions comparables à ceux observés chez les sujets sains. A l'opposé, une diminution de la communication entre les deux zones prédit une évolution défavorable vers un état végétatif ou un état de conscience minimale* ", soulignent Stein Silva et Patrice Péran. Une nouvelle

étude est en cours sur un plus grand nombre de patients (une soixantaine), pour conforter ces observations et analyser plus finement les câblages neuronaux, indique M. Silva.

*" Si ces résultats se confirment, il pourra être utile de proposer une IRM fonctionnelle dans le bilan d'un coma, poursuit le médecin. En outre, cela ouvre des perspectives thérapeutiques, pour tenter de stimuler les connexions chez les patients chez qui l'on observe un potentiel de récupération. "*

*" Pouvoir prédire le plus tôt possible l'évolution de ces malades est un enjeu majeur pour répondre aux questions des familles et prendre des décisions opérationnelles, et ce travail y contribue, se réjouit le - professeur Louis Puybasset, chef du service de neuroréanimation chirurgicale à la Pitié-Salpêtrière, à - Paris. Les recherches de cette équipe sont complémentaires des nôtres, qui évaluent la capacité de récupération des comas par des critères anatomiques comme la qualité de la substance blanche - connexions entre neurones - à l'IRM. "*

**Sandrine Cabut**

© Le Monde

**AUTHOR QUERIES**

DATE 10/26/2015

JOB NAME NEUROLOGY

ARTICLE 2015659672

QUERIES FOR AUTHORS Silva et al

**THIS QUERY FORM MUST BE RETURNED WITH ALL PROOFS FOR CORRECTIONS**

There are no queries in this article.

# Disruption of posteromedial large-scale neural communication predicts recovery from coma

OPEN

Stein Silva, MD, PhD  
Francesco de Pasquale,  
PhD  
Corine Vuillaume, MD  
Beatrice Riu, MD  
Isabelle Loubinoux, PhD  
Thomas Geeraerts, MD,  
PhD  
Thierry Seguin, MD  
Vincent Bounes, MD,  
PhD  
Olivier Fourcade, MD,  
PhD  
Jean-Francois Demonet,  
MD, PhD  
Patrice Péran, PhD

Correspondence to  
Dr. Silva:  
silva.s@chu-toulouse.fr

## ABSTRACT

**Objective:** We hypothesize that the major consciousness deficit observed in coma is due to the breakdown of long-range neuronal communication supported by precuneus and posterior cingulate cortex (PCC), and that prognosis depends on a specific connectivity pattern in these networks.

**Methods:** We compared 27 prospectively recruited comatose patients who had severe brain injury (Glasgow Coma Scale score <8; 14 traumatic and 13 anoxic cases) with 14 age-matched healthy participants. Standardized clinical assessment and fMRI were performed on average  $4 \pm 2$  days after withdrawal of sedation. Analysis of resting-state fMRI connectivity involved a hypothesis-driven, region of interest-based strategy. We assessed patient outcome after 3 months using the Coma Recovery Scale-Revised (CRS-R).

**Results:** Patients who were comatose showed a significant disruption of functional connectivity of brain areas spontaneously synchronized with PCC, globally notwithstanding etiology. The functional connectivity strength between PCC and medial prefrontal cortex (mPFC) was significantly different between comatose patients who went on to recover and those who eventually scored an unfavorable outcome 3 months after brain injury (Kruskal-Wallis test,  $p < 0.001$ ; linear regression between CRS-R and PCC-mPFC activity coupling at rest, Spearman  $\rho = 0.93$ ,  $p < 0.003$ ).

**Conclusion:** In both etiology groups (traumatic and anoxic), changes in the connectivity of PCC-centered, spontaneously synchronized, large-scale networks account for the loss of external and internal self-centered awareness observed during coma. Sparing of functional connectivity between PCC and mPFC may predict patient outcome, and further studies are needed to substantiate this potential prognosis biomarker. *Neurology*® 2015;85:1-9

## GLOSSARY

**BOLD** = blood oxygen level-dependent; **CRS-R** = Coma Recovery Scale-Revised; **DMN** = default-mode network; **FDR** = false discovery rate; **mPFC** = medial prefrontal cortex; **PCC** = posterior cingulate cortex; **PMC** = posteromedial cortex; **PreCu** = precuneus; **ROI** = region of interest; **SMG** = supramarginal gyrus; **TBI** = traumatic brain injury.

Posteromedial cortex (PMC) has traditionally received little attention from neurologists,<sup>1,2</sup> possibly as a consequence of the paucity of focal vascular lesions in this region and its concealed localization. Nevertheless, recent findings suggest that it could have a central role in the regulation of consciousness in humans. First, it has dense structural and functional connections suggesting a role as a cortical hub,<sup>3</sup> an essential property for complex cognitive processes.<sup>4</sup> Second, PMC is also one of the most metabolically active brain regions, both at rest and during self-directed cognition.<sup>5</sup> Third, a selective hypometabolism in this structure has been reported in a wide range of altered consciousness states such as sleep,<sup>6</sup> drug-induced anesthesia,<sup>7</sup> or chronic disorders of consciousness.<sup>8,9</sup> Crucially, in patients with disorders of consciousness, resting-state

Supplemental data  
at [Neurology.org](http://Neurology.org)

From the Critical Care Unit (S.S., B.R.), Critical Care and Anaesthesiology Department (S.S., C.V., B.R., T.G., T.S., O.F.), and SAMU 31 (V.B.), University Teaching Hospital of Purpan, Place du Dr Baylac, F-31059 Toulouse Cedex 9; INSERM U825 (S.S., C.V., I.L., P.P.), CHU Purpan, Place du Dr Baylac, F-31059 Toulouse Cedex 9, France; Department of Radiology (F.d.P.), Santa Lucia Foundation, Rome; ITAB (F.d.P.), Department of Neuroscience Imaging and Clinical Science, G. D'Annunzio University, Chieti, Italy; and Leenaards Memory Center (J.-F.D.), Department of Clinical Neuroscience CHUV and University of Lausanne, Switzerland.

Go to [Neurology.org](http://Neurology.org) for full disclosures. Funding information and disclosures deemed relevant by the authors, if any, are provided at the end of the article. The Article Processing Charge was paid by INSERM.

This is an open access article distributed under the terms of the Creative Commons Attribution-NonCommercial-NoDerivatives License 4.0 (CC BY-NC-ND), which permits downloading and sharing the work provided it is properly cited. The work cannot be changed in any way or used commercially.

functional connectivity with the PMC was found to be correlated with the degree of clinical consciousness impairment across healthy controls and locked-in syndrome to minimally conscious state and vegetative state.<sup>9,10</sup>

The objective of the current study was to investigate the prognostic value of synchronicity indexes of the spontaneous activity in the PMC assessed in a cohort of brain-injured patients at the acute stage of coma. We hypothesized that in the challenging context of coma, the study of brain functional connectivity from PMC might decisively permit to (1) infer the involvement of large-scale functional networks coupled at rest with different PMC subregions (precuneus [PreCu] and posterior cingulate cortex [PCC]) in consciousness generation, (2) identify the functional connectivity patterns that are specifically related to brain injury mechanisms, and (3) explore the extent to which PMC functional connectivity at rest could constitute an early and reliable predictor of neurologic recovery in this setting.

**METHODS Standard protocol approvals, registrations, and patient consents.** This study was approved by the ethics committee of the University Hospital of Toulouse, France (“Comite Consultatif pour la Protection des Personnes,” CHU Toulouse, ID-RCB: 2012-A00009-34). Written informed consent was obtained directly from the healthy volunteers and from the legal surrogate of the patients. Clinical trials identifier: NCT01620957.

**Participants.** This multicenter study was undertaken in 4 intensive critical care units affiliated with the University Teaching Hospital (Toulouse, France) between January 2013 and February 2014. We compared 31 patients with severe brain injury who met the clinical definition of coma (Glasgow Coma Scale score at the admission to hospital <8 with motor responses <6; 16 patients with traumatic and 15 with anoxic brain injury; age range: 23–51 years) with 10 age-matched healthy volunteers (range: 24–45 years). All patients were prospectively recruited and managed according to standard of care recommendations.<sup>11</sup> To avoid confounding factors, all patient assessments were conducted at least 2 days ( $4 \pm 2$  days) after complete withdrawal of sedative drug therapy and performed under normothermic conditions. In patients, standardized clinical examination was performed by raters blinded to neuroimaging data (Glasgow Coma Scale<sup>12</sup> and the Full Outline of Unresponsiveness<sup>13</sup> on the day of scanning and 3 months later using the Coma Recovery Scale–Revised<sup>14</sup>). Table 1 reports demographic and clinical characteristics of the patients.

**Imaging procedures. Acquisitions.** In all participants, 11 minutes of resting-state fMRI was acquired on a 3T magnetic resonance scanner (Intera Achieva; Philips, Best, the Netherlands). Two hundred fifty multislice T2\*-weighted fMRIs were obtained with a gradient echo-planar sequence using axial slice orientation (37 slices; voxel size:  $2 \times 2 \times 3.5$  mm<sup>3</sup>; repetition time = 2,600

milliseconds; echo time = 30 milliseconds; flip angle = 90°; field of view = 240 mm). A 3-dimensional T1-weighted sequence (in-plane resolution  $1 \times 1 \times 1$  mm, 160 contiguous slices) was also acquired in the same session. Monitoring of vital measures was performed by a senior intensivist (S.S., C.V.) throughout the experiment.

**Seed-region integrity.** Two PMC subregions were defined as regions of interest (ROIs): PCC and PreCu (figure e-1 on the *Neurology*<sup>®</sup> Web site at Neurology.org). They covered the entire area of the corresponding anatomical region defined by the Automated Anatomical Labeling atlas.<sup>15</sup> The structural integrity of these seeds was guaranteed by visual assessment on T1 imaging. Four patients (3 with traumatic and 1 with anoxic brain injury) showed significant anatomical anomalies in these regions and were excluded from further analysis. In the remaining participants of the cohort, the T2\* mean values of voxels located in the seed region were extracted from the T2\* mean images and 2-sample *t* tests were performed to compare values measured in the control and patient groups; no significant difference was observed between the groups (table e-1).

**Preprocessing.** Data analysis was performed using SPM8 (<http://www.fil.ion.ucl.ac.uk/spm/>) and the CONN-fMRI functional connectivity toolbox, version 13.p (<http://www.nitrc.org/projects/conn>).<sup>16</sup> Echo-planar images were realigned, coregistered, and normalized to the Montreal Neurological Institute echo-planar imaging template, and smoothed using an 8.0-mm full-width at half maximum isotropic gaussian filter. The head movements estimated during realignment were included in the model as confounding factors. In addition, using the aCompCor method,<sup>17</sup> covariates were included in a principal components analysis (PCA) reduction (3 dimensions) of the signal from white matter and CSF voxels. The residual blood oxygen level–dependent (BOLD) time series was bandpass-filtered over a low-frequency window of interest ( $0.009 \text{ Hz} < f < 0.08 \text{ Hz}$ ).

**Hypothesis-driven–based analysis.** In the first-level analysis, a correlation map was produced for each participant by extracting the residual BOLD time course from each ROI (PreCu and PCC, figure e-1). Pearson correlation coefficients were then calculated between both seed time course and the time course of all other voxels in the brain. Correlation coefficients were converted to normally distributed scores using Fisher transformation to allow for second-level general linear model analyses.

In the second-level analysis, we conducted a within-group analysis (1-sample *t* test) to determine connectivity maps for each group from each ROI. These connectivity maps from each seed ROI from all participants were entered into a 2-sample *t* test, to identify regions with different PCC connectivity or PreCu connectivity across the whole group of patients and healthy controls. We report regions that survived a height threshold of false discovery rate (FDR)-corrected  $p < 0.001$  at the voxel level and an extent threshold of family-wise error–corrected  $p < 0.05$  at the cluster level. We further explored our data until a threshold at FDR-corrected  $p < 0.05$  at the voxel level. The connectivity value (Fisher *z* score) between the seed (PCC and/or PreCu) and each ROI was extracted from the seed connectivity map from each participant, to further segregate between positively vs negatively correlated ROIs relative to each seed region. Fisher *z* values extracted from the ROIs were converted back to correlation coefficients (*r* values) for reporting purposes.

To specifically address the influence of the etiology of brain injury, 3 additional 2-sample *t* tests were conducted on connectivity maps from each seed ROI: patients with traumatic brain injury (TBI) vs controls and anoxic patients vs controls and anoxic vs TBI. Only regions that survived a height threshold of

T1

**Table 1** Population demographics and neurologic outcome

Patient	Sex	Age, y	Etiology	Time to MRI, d	GCS score at scan	FOUR score at scan	CRS-R score at 3 mo	Structural MRI findings
1	M	35	CA	7	7	6	6 (VS)	High signal of the thalami bilaterally
2	M	64	TBI	4	5	5	14 (MCS)	Cortical microhemorrhages (frontal lobes)
3	M	70	CA	5	4	2	4 (VS)	Diffuse hypoxic-ischemic injury (thalami, occipital lobes, parietal lobes)
4	F	58	TBI	3	3	1	9 (VS)	Diffuse axonal injury
5	M	43	TBI	3	4	2	18 (MCS)	Cortical contusions (frontal lobes)
6	M	34	CA	5	4	2	20 (REC)	Mild increase in signal in thalami and hippocampi
7	F	70	TBI	5	5	4	8 (VS)	Cortical contusions (temporal lobes) and subcortical gray matter lesion (thalamus)
8	F	69	TBI	3	5	3	7 (VS)	Diffuse axonal injury
9	M	59	CA	7	6	7	8 (VS)	No abnormality
10	F	19	CA	4	5	5	9 (MCS)	No abnormality
11	F	35	TBI	3	6	5	10 (MCS)	Cortical contusions (parietal lobes) and ventricular enlargement
12	F	48	CA	5	3	1	15 (MCS)	Diffuse ischemic changes (thalami, occipital lobes)
13	M	59	TBI	2	4	4	16 (MCS)	Cortical, brainstem and cerebellar lesions
14	F	47	CA	5	5	6	8 (VS)	No abnormality
15	M	56	TBI	3	5	5	6 (VS)	Diffuse axonal injury and brainstem lesion
16	M	56	TBI	4	6	6	21 (REC)	Cortical contusions
17	F	35	CA	6	5	4	22 (REC)	High signal in thalami bilaterally
18	M	58	CA	6	6	5	7 (VS)	No abnormality
19	F	39	CA	7	7	6	12 (MCS)	No abnormality
20	M	43	TBI	5	5	6	14 (MCS)	Diffuse axonal injury
21	M	20	TBI	3	6	7	6 (VS)	Diffuse axonal injury
22	M	52	TBI	4	6	7	5 (VS)	Brainstem and cerebellar lesions
23	F	53	CA	5	5	4	9 (VS)	High signal of the thalami bilaterally
24	M	25	CA	5	6	6	12 (MCS)	No abnormality
25	M	21	TBI	6	6	5	14 (MCS)	Cortical contusions (temporal lobes) and diffuse axonal injury
26	F	58	TBI	9	6	7	23 (REC)	Cortical contusions (frontal lobes)
27	M	49	CA	8	5	4	13 (MCS)	High increase in signal in thalami and hippocampi

Abbreviations: CA = cardiac arrest; CRS-R = Coma Recovery Scale-Revised; FOUR = Full Outline of Unresponsiveness; GCS = Glasgow Coma Scale; MCS = minimally conscious state; TBI = traumatic brain injury; VS = vegetative state.

FDR-corrected  $p < 0.001$  at the voxel level and an extent threshold of family-wise error-corrected  $p < 0.05$  at the cluster level were reported. Finally, a null conjunction was performed between TBI vs controls and anoxic vs controls. We used FDR correction with  $p < 0.05$  at a voxel level.

Behavioral data are expressed as median and range. Data distributions were compared with Kruskal-Wallis test, and the statistical dependence between 2 variables was assessed using Spearman rank correlation coefficient.

**Data-driven analysis.** To provide an additional methodologic control, we included a complementary data-driven spatial independent component analysis<sup>18</sup> to decompose data into statistically independent spatial and temporal components<sup>19</sup> (<http://icatb.sourceforge.net>). A standard template of the default-mode network (DMN) was used to identify network components

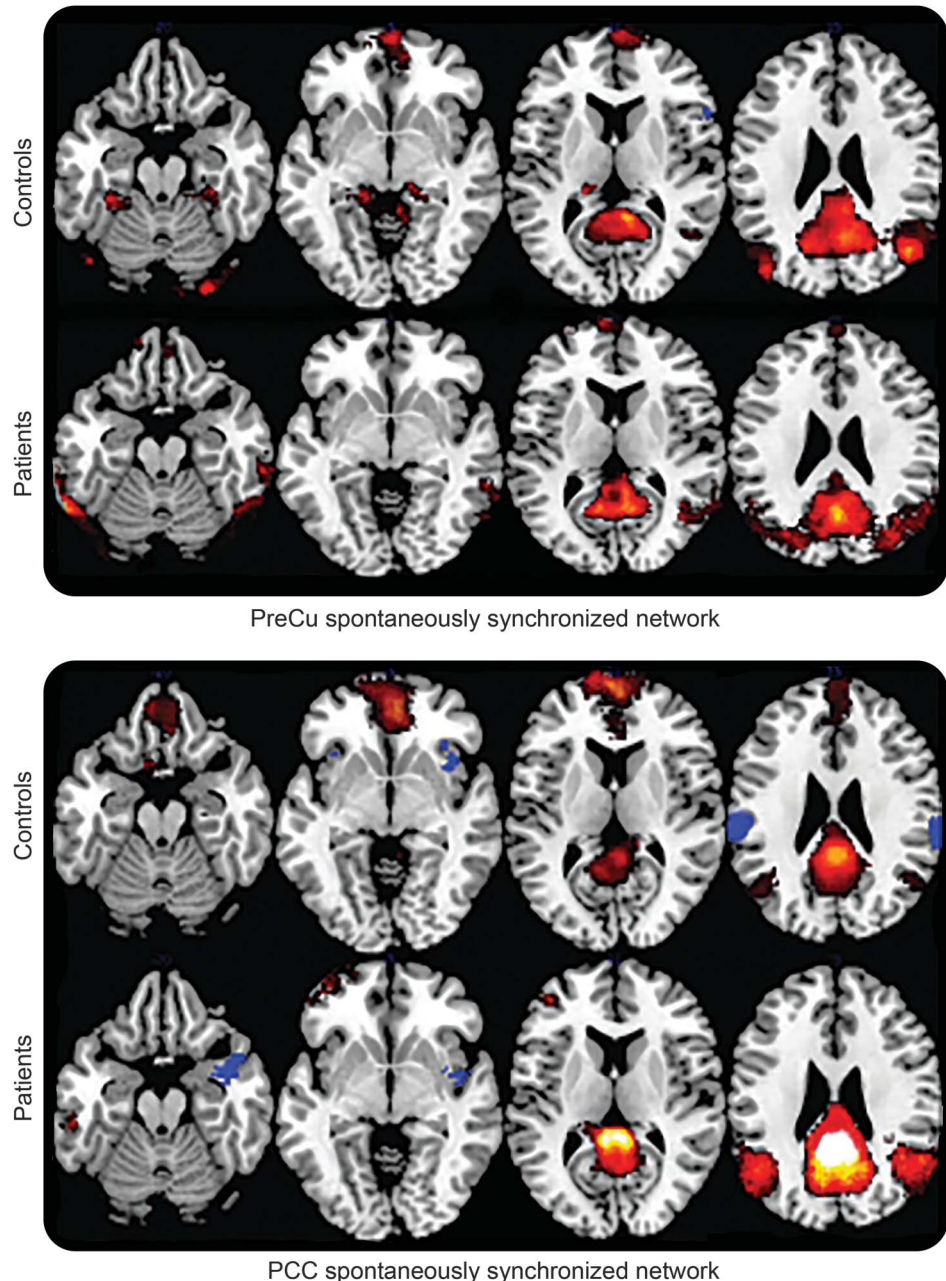
on a subject-by-subject basis.<sup>20</sup> SPM8 (<http://www.fil.ion.ucl.ac.uk/spm/>) was used for the statistical comparison of images. These ancillary data have been used to create figure e-2.

## RESULTS Plasticity of brain connections after injury.

In figure 1, we report group-level results of seed-based connectivity analyses obtained when PreCu and PCC were considered in turn as seed. The obtained comatose patient's topography resembled the one reported in healthy controls, involving correlated brain areas (figure 1, red) previously described as being part of internally directed cognition networks<sup>21</sup>: medial prefrontal cortex (mPFC), temporoparietal junction, and parahippocampal and superior frontal gyri. In

F1

**Figure 1** Large-scale spontaneously synchronized networks



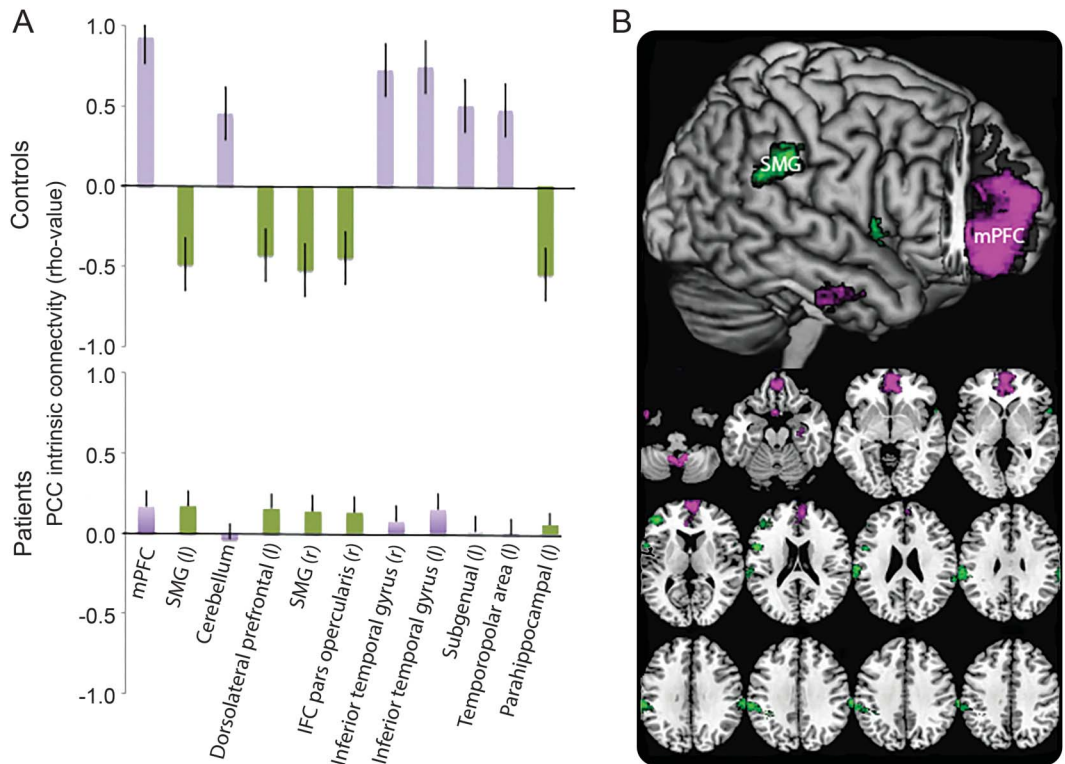
Whole-brain functional connectivity maps of covariance were computed in both groups (i.e., comatose patients and controls) following a hypothesis-driven approach. Two seed-based structures were analyzed: posterior cingulate cortex (PCC) and precuneus (PreCu). Color intensity depicts level of synchronicity (red and blue for positive and negative temporal signals correlations, respectively). All  $p$  values are corrected for false discovery rate at the whole brain level ( $p$  value  $<0.0001$ , corrected for false discovery rate).

addition, we also observed in both patient and control groups a set of brain areas that were spontaneously anticorrelated with PCC and PreCu (figure 1, blue). Such anticorrelated network bilaterally involved the supramarginal gyrus (SMG) and the insulae, regions that are known to take part in networks supporting externally directed cognition.<sup>22</sup>

In addition, to quantify the observational similarity between healthy control and patient connectivity

maps, we computed the statistical differences between the obtained networks (figure 2, in purple and green significant positive and negative differences, respectively). When considering PCC as seed region, we observed a significant and specific functional connectivity change in patients who were comatose relative to healthy controls (figure 2A). It is worth noting that these functional connectivity disruptions from PCC involved spontaneously correlated (e.g., mPFC) and

**Figure 2** Comparison between intrinsic PCC synchronized networks identified in patients who were comatose and controls



(A) Color intensity depicts differences of synchronicity between both groups (purple and green for positive and negative differences, respectively). (B) Spatial distribution of differences of temporal synchronicity values between patients and controls. All  $p$  values are corrected for false discovery rate at the whole brain level ( $p$  value  $< 0.0001$ , corrected for false discovery rate). IFC = inferior frontal cortex; mPFC = mesial prefrontal cortex (BA9); PCC = posterior cingulate cortex; SMG = supramarginal gyrus (BA40).

anticorrelated (e.g., SMG) brain areas (figure 2B). A data-driven spatial independent component analysis, used as a methodologic control, confirms that DMN was indeed much less integrated in patients who were comatose compared with controls (figure e-2).

In contrast, no such group differences were observed for connectivity of the PreCu seed region ( $p < 0.05$ , FDR-corrected), suggesting the preservation of a global cortical network orchestrated by Pre-Cu over time in resting state during coma.

**Effect of brain injury mechanism.** It is worth noting that no difference was found between the resting-state networks obtained from patients of traumatic vs anoxic origin at the defined statistical threshold ( $p < 0.05$ , FDR-corrected). Using a lower threshold ( $p < 0.001$ , uncorrected), only 2 clusters of voxel were identified: the left somatosensory associative cortex (BA7) and the retrosplenial cingulate cortex (BA29). Of note, largely overlapping networks were observed when comparing intrinsic connectivity networks from coma patients of traumatic vs anoxic origin (figure 3). A conjunction analysis confirmed and extended this finding (figure e-3), suggesting a common pattern of neural communication disturbance in coma patients,

notwithstanding etiology. To summarize, we observed at the same level, in both traumatic and anoxic patients, a significant disturbance in coactivation of distant regions from PCC, in particular with the midline forebrain areas.

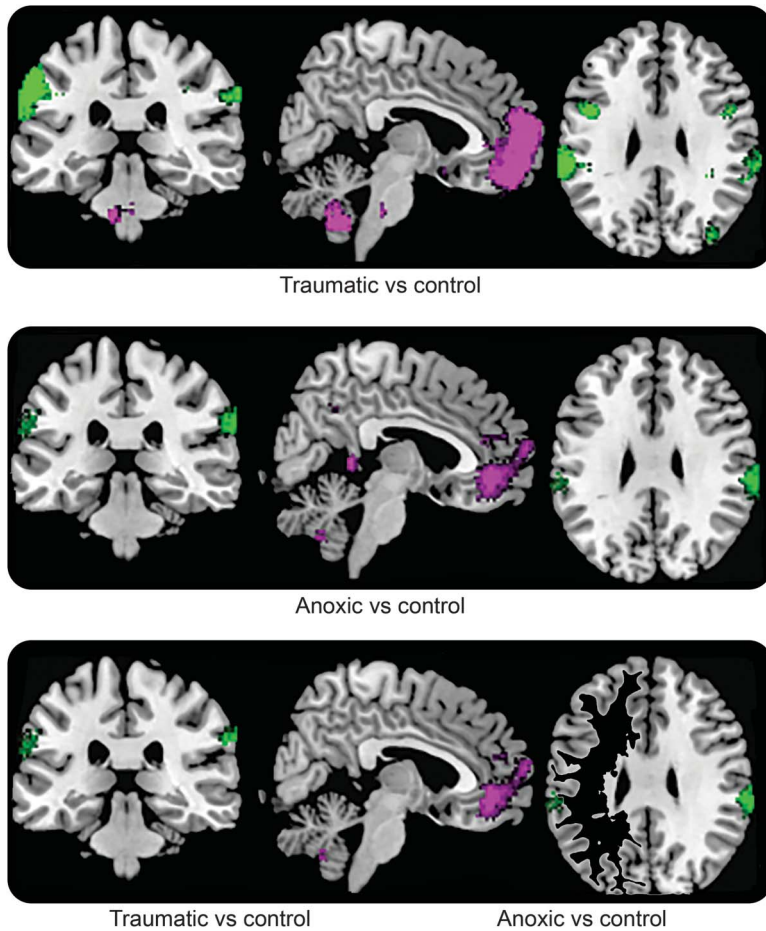
**Prognostic value.** In this behaviorally homogeneous cohort of patients who were comatose (table 1), we observed that the functional connectivity strength between PCC-mPFC assessed at the acute stage where patients were scanned, was significantly different between comatose patients who went on to recover and those who eventually scored an unfavorable outcome 3 months after the brain injury (figure 4A). In addition, the linear regression between patients' outcome score on CRS-R and the PCC-mPFC activity coupling at rest substantiated a significant link between PCC-mPFC functional connectivity that was recorded promptly after brain injury and patients' neurologic recovery evaluated later (figure 4B).

**DISCUSSION** Theoretical conceptualizations of the neural bases of conscious processes suggest that both local and long-range recursive processing loops through cortical hubs permit global availability of

F3

F4

**Figure 3** Intrinsic PCC synchronized networks identified in comatose patients with anoxic and traumatic injury compared with controls



One seed-based structure was analyzed (PCC) ( $p$  value  $<0.0001$ , corrected for false discovery rate). Both etiologic subgroups are represented (i.e., traumatic and anoxic mechanism, upper and middle panel, respectively). In addition, overlapping resting-state networks, in which activity is spontaneously synchronized with PCC in both traumatic and anoxic comatose patients compared with controls, are depicted in the lower panel. PCC = posterior cingulate cortex.

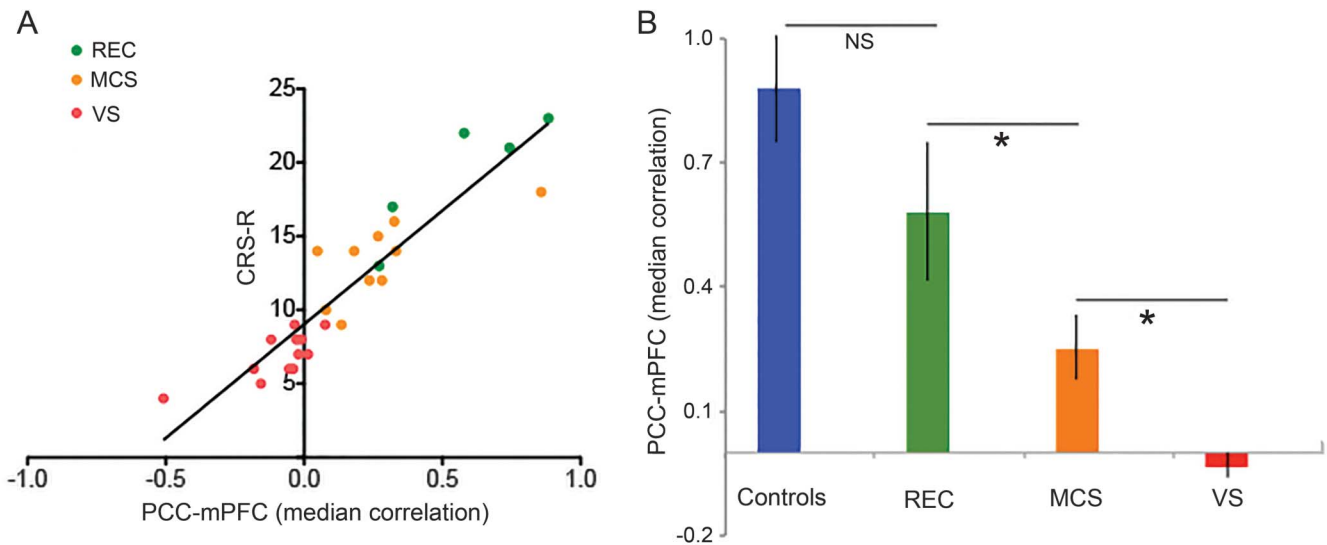
information throughout key cortical regions; it is believed that such a global neural workspace<sup>4</sup> is the substrate of consciousness. In line with this theoretical framework, our findings suggest that the neural underpinnings of the pathologic alteration of consciousness named coma consist of disruption of the large-scale brain network involving key regions such as PCC and mPFC. Of note, we found that acute brain injuries responsible for coma yield a reorganization of existing intrinsic brain networks rather than a complete annihilation. At variance with a previous study suggesting that coma induced a dichotomic all-or-nothing distribution of resting-state networks,<sup>18</sup> we found that spontaneous synchronized brain activity as a whole was maintained during coma; yet, contributions of the PCC to the network were specifically decreased. In this challenging clinical setting, we found that functional connectivity strength between PCC and mPFC, recorded at the acute stage of

coma, has a significant predictive value of further neurologic recovery. Our results support previous reports suggesting that cortico-cortical spontaneous synchronization may be used as an efficient diagnostic classifier for vegetative state and minimally conscious state<sup>8,9</sup> and pave the way for future longitudinal studies aiming to fully describe the structural and functional network dysfunction induced by severe brain injury from acute comatose states throughout the recovery phase.

It must be highlighted that most of the studies that have analyzed the functional contribution of the PMC in patients with acquired disorders of consciousness explored this portion of the parietal lobe as an indivisible structure (PCC/PreCu).<sup>8,9,18,23</sup> Nevertheless, a growing body of research has suggested an important structural and functional heterogeneity within this large region. Cytoarchitecturally, the PCC is characterized as paralimbic cortex, exhibiting a transitional cell architecture organized in 2 subregions, one dorsal (areas d23a, d23b, 23d, anterior 31) and one ventral (v23a and v23b, posterior 31).<sup>24</sup> In addition, tract-tracing studies conducted in nonhuman primates<sup>25</sup> and diffusion-tensor tractography in humans<sup>26</sup> have clearly identified structural connections between the ventral PCC and the medial temporal lobes, as well as connections from more dorsal PCC to the mPFC along the cingulum bundle.<sup>27</sup> Finally, PCC complex cognitive function has been recently synthesized into an “Arousal, Balance of Breath of Attention” model.<sup>2</sup> However, PreCu (BA7) is characterized by a fully differentiated isocortex,<sup>28</sup> has reciprocal cortico-cortical connections with the adjacent areas of the PMC, namely, the frontal lobes, the supplementary motor area,<sup>29</sup> together with its own major subcortical connections with the basal ganglia and the brainstem.<sup>30</sup> Functional neuroimaging studies appear to converge with evidence for a functional role of PreCu involving self-centered imagery strategies and subserving successful episodic memory retrieval.<sup>31</sup> Our data are in line with this PMC heterogeneity, since we found significant differences of connectivity changes between intrinsic networks depending on whether the considered seed region was PCC or PreCu.

Regarding the temporally coupled networks seeded in PCC at rest, we identified a 2-fold connectivity disruption pattern. First, we observed a midline decoupling of PCC and mPFC suggesting network sensitivity to changes in level of consciousness. Of note, our results agree with previous reports suggesting a link between internal awareness and the activity of mPFC and PCC,<sup>22</sup> as a stepwise reduction of connectivity between these midline structures in different sleep states<sup>6</sup> and loss of the normal top-down cortico-cortical communication between them observed with

**Figure 4** Predictive role of PCC-mPFC coupling measured during coma state and neurologic outcome



The linear regression between patient outcome CRS-R and early-recorded PCC-mPFC coupling at rest (A) suggested a significant link between PCC-mPFC functional connectivity and patient neurologic recovery (Spearman  $\rho = 0.93$ ,  $p < 0.003$ ). Functional connectivity strength between PCC-mPFC assessed at scan time (B) was significantly different between comatose patients who recovered consciousness (REC) and those who evolved toward a minimally conscious state (MCS) or a vegetative state (VS) 3 months after the brain injury (Kruskal-Wallis test,  $p < 0.001$ ). PCC-mPFC synchronicity at rest was not different between REC and controls. mPFC = medial prefrontal cortex; NS = not significant; PCC = posterior cingulate cortex.

propofol sedation.<sup>32</sup> This finding is also convergent with the hypothesis of a dysfunctional mesocircuit,<sup>33</sup> which posits that the anterior forebrain function is markedly downregulated in all severe brain injuries as a result of long-range cerebral disconnections. Second, we detected in patients a deficit of the normal correlation over time between PCC and lateral parietal cortices (mainly SMG) that have been previously associated with external awareness.<sup>34</sup> We suggest that our data could depict breakdown of the dynamic reciprocal interaction between internal and external awareness systems during coma and highlight the pivotal role of PCC for “tuning” the whole-brain metastable status.<sup>35</sup>

Remarkably, the alteration of coordination over time between PCC and midline forebrain areas was found to be at a similar level in both patients with traumatic and patients with anoxic injury. Converging structural neuroimaging data have shown specific perturbations of white matter pathways between PCC and mPFC in both traumatic brain injury<sup>36</sup> and anoxia.<sup>37</sup> However, we submit the alternative and complementary account according to which the anterior–posterior disconnection pattern jointly observed in both anoxic and traumatic groups reflects remote and diffuse functional imbalance throughout the whole neuronal system (i.e., diaschisis). Future studies combining structural and functional data will be needed to specifically address this issue.

The measurement of PreCu spontaneous activity synchronicity at rest, compared between patients

who were comatose and controls allowed us to identify a robust and autonomous intrinsic network, encompassing the areas implicated in the DMN. We observed that even in this extreme pathologic condition of consciousness disruption, the functional architecture of this PreCu-based network as a whole was maintained. This important point could be contextualized with the experimental background suggesting that the DMN may be needed for consciousness to occur but is not sufficient on its own to elicit awareness.<sup>38</sup> It seems that this functional connectivity pattern linked to PreCu spontaneous activity transcends the level of consciousness, and could probably be considered as a physiologic baseline.

Several limitations of our study should be recognized. First, the number of patients is relatively small and our results need to be prospectively validated in larger cohorts. Second, there is a possibility that our fMRI findings could change depending on the time of scanning in relation to the time of injury.<sup>18</sup> This important point highlights the interest of early and repeated neuroimaging assessments in this setting, intended to accurately identify and monitor the brain network functional changes that are specifically related to consciousness emergence from coma.

To summarize, the reorganization of PCC-centered, spontaneously synchronized, large-scale networks seems to be implicated in the loss of external and internal self-centered awareness observed during coma, largely independent of its etiology. The level of functional connectivity between PCC and mPFC appears to be related

to patient neurologic outcome. Future work should further explore brain intrinsic network dysfunctions in larger patient cohorts, aiming to improve patient diagnosis and early prognostication and enable the development of innovative network-based personalized treatments.

### AUTHOR CONTRIBUTIONS

S.S. takes responsibility for the content of the manuscript, including the data and analysis. He conceived the study and has personally made contributions to the design of the study, the acquisition of data, and the analysis and interpretation of data. C.V., B.R., T.G., T.S., V.B., and O.F. have substantially participated in the data acquisition. P.P. and I.L. have made contribution to the design of the study. P.P., F.d.P., and J.-F.D. have contributed to the conception and analysis of data. S.S., F.d.P., J.-F.D., and P.P. wrote the manuscript. All authors have revised the submitted manuscript critically for important intellectual content and they have provided final approval of this version to be published. All authors agree to the conditions outlined in the Guide for Authors.

### ACKNOWLEDGMENT

The authors thank the technicians and engineers of the Neurocampus and Brain Imaging Center of Purpan (Helene Gros, Nathalie Vayssiere) and the medical staff of the Critical Care Units of the University Teaching Hospital of Toulouse (Mylene Terrade, Fanny Vardon, Lionel Kheruel, Dalinda Ait Aissa) for their active participation in the MRI studies in comatose patients.

### STUDY FUNDING

Funding was provided by the Association des Traumatisés du Crâne et de la Face, Institut des Sciences du Cerveau de Toulouse, and Institut National de la Santé et de la Recherche Médicale. The funding sources had no role in the study design, data collection, data analysis, data interpretation, or writing of this report.

### DISCLOSURE

The authors report no disclosures relevant to the manuscript. Go to [Neurology.org](http://Neurology.org) for full disclosures.

*Received April 8, 2015. Accepted in final form August 10, 2015.*

### REFERENCES

1. Cavanna AE, Trimble MR. The precuneus: a review of its functional anatomy and behavioural correlates. *Brain* 2006;129:564–583.
2. Leech R, Sharp DJ. The role of the posterior cingulate cortex in cognition and disease. *Brain* 2014;137:12–32.
3. Andrews-Hanna JR, Reidler JS, Sepulcre J, Poulin R, Buckner RL. Functional-anatomic fractionation of the brain's default network. *Neuron* 2010;65:550–562.
4. Dehaene S, Changeux JP. Experimental and theoretical approaches to conscious processing. *Neuron* 2011;70:200–227.
5. Gusnard DA, Akbudak E, Shulman GL, Raichle ME. Medial prefrontal cortex and self-referential mental activity: relation to a default mode of brain function. *Proc Natl Acad Sci USA* 2001;98:4259–4264.
6. Horowitz SG, Braun AR, Carr WS, et al. Decoupling of the brain's default mode network during deep sleep. *Proc Natl Acad Sci USA* 2009;106:11376–11381.
7. Amico E, Gomez F, Di Perri C, et al. Posterior cingulate cortex-related co-activation patterns: a resting state fMRI study in propofol-induced loss of consciousness. *PLoS One* 2014;9:e100012.
8. Silva S, Alacoque X, Fourcade O, et al. Wakefulness and loss of awareness: brain and brainstem interaction in the vegetative state. *Neurology* 2010;74:313–320.
9. Vanhaudenhuyse A, Noirhomme Q, Tshibanda LJ, et al. Default network connectivity reflects the level of consciousness in non-communicative brain-damaged patients. *Brain* 2010;133:161–171.
10. Soddu A, Vanhaudenhuyse A, Demertzi A, et al. Resting state activity in patients with disorders of consciousness. *Funct Neurol* 2011;26:37–43.
11. Menon DK. Cerebral protection in severe brain injury: physiological determinants of outcome and their optimization. *Br Med Bull* 1999;55:226–258.
12. Plum F, Posner J. *The Diagnosis of Stupor and Coma*. Philadelphia: F.A. Davis; 1982.
13. Wijdicks EF, Bamlet WR, Maramattom BV, Manno EM, McClelland RL. Validation of a new coma scale: the FOUR score. *Ann Neurol* 2005;58:585–593.
14. Boly M, Massimini M, Tononi G. Theoretical approaches to the diagnosis of altered states of consciousness. *Prog Brain Res* 2009;177:383–398.
15. Tzourio-Mazoyer N, Landeau B, Papathanassiou D, et al. Automated anatomical labeling of activations in SPM using a macroscopic anatomical parcellation of the MNI MRI single-subject brain. *Neuroimage* 2002;15:273–289.
16. Whitfield-Gabrieli S, Nieto-Castanon A. Conn: a functional connectivity toolbox for correlated and anticorrelated brain networks. *Brain Connect* 2012;2:125–141.
17. Behzadi Y, Restom K, Liu J, Liu TT. A component based noise correction method (CompCor) for BOLD and perfusion based fMRI. *Neuroimage* 2007;37:90–101.
18. Norton L, Hutchison RM, Young GB, Lee DH, Sharpe MD, Mirsattari SM. Disruptions of functional connectivity in the default mode network of comatose patients. *Neurology* 2012;78:175–181.
19. Calhoun VD, Adali T, Pearlson GD, Pekar JJ. A method for making group inferences from functional MRI data using independent component analysis. *Hum Brain Mapp* 2001;14:140–151.
20. Garrity AG, Pearlson GD, McKiernan K, Lloyd D, Kiehl KA, Calhoun VD. Aberrant “default mode” functional connectivity in schizophrenia. *Am J Psychiatry* 2007;164:450–457.
21. Raichle ME, MacLeod AM, Snyder AZ, Powers WJ, Gusnard DA, Shulman GL. A default mode of brain function. *Proc Natl Acad Sci USA* 2001;98:676–682.
22. Dixon ML, Fox KC, Christoff K. A framework for understanding the relationship between externally and internally directed cognition. *Neuropsychologia* 2014;62:321–330.
23. Laureys S, Goldman S, Phillips C, et al. Impaired effective cortical connectivity in vegetative state: preliminary investigation using PET. *Neuroimage* 1999;9:377–382.
24. Vogt BA, Laureys S. Posterior cingulate, precuneal and retrosplenial cortices: cytology and components of the neural network correlates of consciousness. *Prog Brain Res* 2005;150:205–217.
25. Vogt BA, Vogt L, Farber NB, Bush G. Architecture and neurocytology of monkey cingulate gyrus. *J Comp Neurol* 2005;485:218–239.
26. Hagmann P, Cammoun L, Gigandet X, et al. Mapping the structural core of human cerebral cortex. *PLoS Biol* 2008;6:e159.
27. Greicius MD, Supekar K, Menon V, Dougherty RF. Resting-state functional connectivity reflects structural connectivity in the default mode network. *Cereb Cortex* 2009;19:72–78.

28. Pandya DN, Seltzer B. Intrinsic connections and architectonics of posterior parietal cortex in the rhesus monkey. *J Comp Neurol* 1982;204:196–210.
29. Cavada C, Goldman-Rakic PS. Posterior parietal cortex in rhesus monkey: I: parcellation of areas based on distinctive limbic and sensory corticocortical connections. *J Comp Neurol* 1989;287:393–421.
30. Petrides M, Pandya DN. Projections to the frontal cortex from the posterior parietal region in the rhesus monkey. *J Comp Neurol* 1984;228:105–116.
31. Fletcher PC, Frith CD, Baker SC, Shallice T, Frackowiak RS, Dolan RJ. The mind's eye: precuneus activation in memory-related imagery. *Neuroimage* 1995;2:195–200.
32. Boly M, Moran R, Murphy M, et al. Connectivity changes underlying spectral EEG changes during propofol-induced loss of consciousness. *J Neurosci* 2012;32:7082–7090.
33. Schiff ND. Recovery of consciousness after brain injury: a mesocircuit hypothesis. *Trends Neurosci* 2010;33:1–9.
34. Vanhaudenhuyse A, Demertzi A, Schabus M, et al. Two distinct neuronal networks mediate the awareness of environment and of self. *J Cogn Neurosci* 2011;23:570–578.
35. Hellyer PJ, Shanahan M, Scott G, Wise RJ, Sharp DJ, Leech R. The control of global brain dynamics: opposing actions of frontoparietal control and default mode networks on attention. *J Neurosci* 2014;34:451–461.
36. Palacios EM, Sala-Llonch R, Junque C, et al. White matter/gray matter contrast changes in chronic and diffuse traumatic brain injury. *J Neurotrauma* 2013;30:1991–1994.
37. Luyt CE, Galanaud D, Perlberg V, et al. Diffusion tensor imaging to predict long-term outcome after cardiac arrest: a bicentric pilot study. *Anesthesiology* 2012;117:1311–1321.
38. Vincent JL, Patel GH, Fox MD, et al. Intrinsic functional architecture in the anesthetized monkey brain. *Nature* 2007;447:83–86.



# Polarized cellular patterns of endocannabinoid production and detection shape cannabinoid signaling in neurons

Delphine Ladarre<sup>1,2</sup>, Alexandre B. Roland<sup>1,2†</sup>, Stefan Biedzinski<sup>1,2</sup>, Ana Ricobaraza<sup>1,2</sup> and Zsolt Lenkei<sup>1,2\*</sup>

<sup>1</sup> Brain Plasticity Unit, ESPCI-ParisTech, Paris, France

<sup>2</sup> Centre National de la Recherche Scientifique UMR 8249, Paris, France

## Edited by:

Pierre Vincent, Centre National de la Recherche Scientifique, France

## Reviewed by:

Thomas Launey, RIKEN, Japan  
Xiang Yu, The Chinese Academy of Sciences, China

## \*Correspondence:

Zsolt Lenkei, Brain Plasticity Unit, ESPCI-ParisTech, 10, rue Vauquelin, 75005 Paris, France  
e-mail: zsolt.lenkei@espci.fr

## † Present address:

Alexandre B. Roland, FAS Center for Systems Biology, Harvard University, Cambridge, MA, USA

Neurons display important differences in plasma membrane composition between somatodendritic and axonal compartments, potentially leading to currently unexplored consequences in G-protein-coupled-receptor signaling. Here, by using highly-resolved biosensor imaging to measure local changes in basal levels of key signaling components, we explored features of type-1 cannabinoid receptor (CB1R) signaling in individual axons and dendrites of cultured rat hippocampal neurons. Activation of endogenous CB1Rs led to rapid,  $G_{i/o}$ -protein- and cAMP-mediated decrease of cyclic-AMP-dependent protein kinase (PKA) activity in the somatodendritic compartment. In axons, PKA inhibition was significantly stronger, in line with axonally-polarized distribution of CB1Rs. Conversely, inverse agonist AM281 produced marked rapid increase of basal PKA activation in somata and dendrites, but not in axons, removing constitutive activation of CB1Rs generated by local production of the endocannabinoid 2-arachidonoylglycerol (2-AG). Interestingly, somatodendritic 2-AG levels differently modified signaling responses to CB1R activation by  $\Delta^9$ -THC, the psychoactive compound of marijuana, and by the synthetic cannabinoids WIN55,212-2 and CP55,940. These highly contrasted differences in sub-neuronal signaling responses warrant caution in extrapolating pharmacological profiles, which are typically obtained in non-polarized cells, to predict *in vivo* responses of axonal (i.e., presynaptic) GPCRs. Therefore, our results suggest that enhanced comprehension of GPCR signaling constraints imposed by neuronal cell biology may improve the understanding of neuropharmacological action.

**Keywords: CB1, DAGL, endocannabinoid, cyclic nucleotide, allosteric, biased agonism, lipid, FRET**

## INTRODUCTION

Polarized neuronal architecture maintains the directionality of information flow through neuronal networks. Accordingly, protein and lipid composition of the plasma membrane greatly differs between axons and the somatodendritic compartment (Horton and Ehlers, 2003). Local interaction between cell membrane components is increasingly considered as a key dynamic component in sensory and signaling pathways. Notably, the highly regulated lipid environment may control the structure, conformation and function of embedded proteins (Phillips et al., 2009). A major brain G-protein coupled receptor (GPCR) that may be particularly sensitive to the lipid composition of the plasma membrane is the type-1 cannabinoid receptor (CB1R). Predominantly localized in axons and specific presynaptic nerve terminals, CB1R is the neuronal target of endocannabinoid lipids (eCBs) and of  $\Delta^9$ -tetrahydrocannabinol (THC), the major psychoactive substance of marijuana. CB1Rs may show elevated tonic (constitutive) activation in neurons (Pertwee, 2005), potentially resulting from a combined effect of conformational instability (D'Antona et al., 2006) and ubiquitously present membrane-borne eCBs, such as 2-arachidonoylglycerol (2-AG), which is the most prominent brain eCB (Alger and Kim, 2011; Howlett et al.,

2011) as well as an important intermediate in the production of several other bioactive lipids (Nomura et al., 2011). 2-AG is released from cell membrane phospholipids by the action of phospholipase C and diacylglycerol lipases (DAGL $\alpha$  and DAGL $\beta$ ). eCBs are generally considered to be retrograde signals, being produced in the postsynaptic cell and traveling “backwards” across the synaptic cleft to activate CB1Rs on presynaptic nerve terminals (Freund et al., 2003; Kano et al., 2009). However, in addition to this retrograde synaptic signaling effect, eCBs synthesized in the somatodendritic membrane may also have cell-autonomous effects on local CB1Rs, such as endocannabinoid-mediated somatodendritic slow self-inhibition (SSI) (Bacci et al., 2004; Marinelli et al., 2009) or somatodendritic endocytosis-driven transcytotic targeting (Leterrier et al., 2006; Simon et al., 2013). These findings suggest that locally produced 2-AG may activate somatodendritic CB1Rs, although such CB1R-induced somatodendritic signaling has not yet been shown directly.

CB1R activation, through coupling to  $G_{i/o}$  heterotrimeric proteins, leads to inhibition of cyclic adenosine monophosphate (cAMP) production and inhibition of cyclic-AMP-dependent protein kinase (PKA) activity (Howlett, 2005). cAMP and PKA regulate essential biological functions in neurons such

as excitability, efficacy of synaptic transmission and axonal growth/pathfinding. Therefore, CB1R coupling to this major signaling pathway may have important consequences on neuronal function. However, in absence of direct measurement of somatodendritic and axonal CB1R signaling, whether and how differences in local CB1R density and local 2-AG content regulate signaling responses to cannabinoids remain unknown.

More generally, it is currently not known how the highly-polarized neuronal membrane environment may shape GPCR signaling. This information may be important to better understand neuronal effects of therapeutic or abused drugs. Indeed, pharmacological response profiles are usually established in non-polarized heterologous expression systems, such as immortalized cell lines, but results derived from these experimental setups may not precisely indicate the pharmacological response that the studied ligand will elicit in polarized neuronal environments, for instance in the extremely thin axons. Therefore, here we used a highly-resolved and sensitive Förster Resonance Energy Transfer (FRET) approach to measure *in vitro* ligand-induced modulation of basal cAMP/PKA levels downstream of endogenous CB1Rs, in individual axons, dendrites, and somata of well-differentiated hippocampal neurons.

## MATERIALS AND METHODS

### ANIMALS

All experiments were performed in agreement with the European Community Council Directive of 22nd September 2010 (010/63/UE) and the local ethics committee (*Comité d'éthique en matière d'expérimentation animale n° 59, C2EA – 59, 'Paris Centre et Sud'*) were used for dissociated cell culture experiments.

### CHEMICALS, ANTIBODIES AND DNA CONSTRUCTS

CB1R agonists WIN55,212,2 (WIN), CP55,940 (CP) and 2-arachidonoylglycerol (2-AG), CB1R inverse agonist AM281 (AM) and DAGL inhibitor RHC80267 (RHC) were obtained from R&D Systems Europe. Dimethyl Sulfoxide (DMSO), Tetrahydropyridinylpiperazine (THL),  $\Delta^9$ -Tetrahydrocannabinol solution (THC), Pertussis Toxin (PTX), Forskolin (Fsk), monoclonal mouse anti-Tau antibody, monoclonal mouse anti-microtubule-associated protein 2 (anti-MAP2) antibody, Bovine Serum Albumin (BSA) and Poly-D-Lysine were obtained from SIGMA-ALDRICH. Polyclonal anti-DAGL $\alpha$  antibody was obtained from Frontier Institute co., Ltd (JAPAN). B27, Lipofectamine 2000 and Neurobasal were obtained from Life Technologies.

AKAR4, Lyn-AKAR4 and AKAR4-Kras probes were provided by Dr. Jin Zhang's laboratory (Baltimore, USA). <sup>T</sup>Epac<sup>vv</sup> probe provided by Dr. Kees Jalink laboratory (Amsterdam, Netherlands).

### HIPPOCAMPAL NEURONAL CULTURES

Hippocampal neuronal cultures were performed essentially as described previously (Letierrier et al., 2006). Briefly, hippocampi of Sprague–Dawley rat (Janvier) embryos were dissected at embryonic day 18. After trypsinization, dissociation was achieved with a fire-polished Pasteur pipette. Cells were counted and plated on poly-D-lysine-coated 18-mm diameter glass coverslips, at a density of 300–400 cells/mm<sup>2</sup>. The plating medium was

Neurobasal supplemented with 2% B27 and containing Stabilized Glutamine (0.5 mM) and penicillin G (10 U/ml)/streptomycin (10 g/ml). Four hours after plating, the coverslips were transferred into Petri dishes containing supplemented Neurobasal medium that had been conditioned for 24 h on a 80% confluent glia layer. Neurons were transfected after 6 days *in vitro* (DIV6) using Lipofectamine 2000, following the manufacturer's instructions.

### FRET IMAGING

Neurons transfected either with <sup>T</sup>Epac<sup>vv</sup> or AKAR4-Kras probes were imaged by videomicroscopy between DIV7 and DIV11 on a motorized Nikon Eclipse Ti-E/B inverted microscope with the Perfect Focus System (PFS) in a 37°C thermostated chamber, using an oil immersion CFI Plan APO VC 60X, NA 1.4 objective (Nikon).

Acquisitions were carried out at the excitation wavelength of the CFP (434 ± 15 nm) using an Intensilight (Nikon). Emitted light passed through an Optosplit II beam-splitter (Cairn Research) equipped with a FF509-FD101 dichroic mirror, a FF01-483/32-25 CFP filter and a FF01-542/27-25 YFP filter and was collected by an EM-CCD camera (Evolve 512, Photometrics), mounted behind a 2× magnification lens. Acquisitions were performed by piloting the set-up with Metamorph 7.7 (Molecular Devices). All filter sets were purchased from Semrock.

Cultured neurons on 18-mm coverslips were placed in a closed imaging chamber containing an imaging medium: 120 mM NaCl, 3 mM KCl, 10 mM HEPES, 2 mM CaCl<sub>2</sub>, 2 mM MgCl<sub>2</sub>, 10 mM D-glucose, 2% B27, 0.001% BSA.

We have previously characterized axons and dendrites in our cultures by using immunolabeling for Tau and MAP2 proteins, respectively, that allowed to establish the characteristic morphology of these neurites in cultured hippocampal neurons. Here we have used this morphological criteria to identify axons and dendrites. The acquisition lasted 90 min, recording one image each 2 min, by imaging in parallel 25–30 [10 à 15 neurones mais pour chaque neurone: 1 champs sur soma, 1 champ sur l'axone et une champ sur dendrites distales (facultatif)] fields-of view on the same coverslip. 30 min after the beginning of the acquisition, pharmacological treatment was applied then 60 min after the beginning of the acquisition, Forskolin 10 μM was applied.

### FRET DATA ANALYSIS

All imaged neurons were analyzed and included in the final result, except the neurons that matched at least one of the three pre-defined exclusion criteria: (1) lack of response to the terminal Fsk stimulation, (2) loss of focus during the time-lapse sequence, or (3) the impossibility to realign artifactual lateral movement. All key analysis results were obtained by an experimenter blind to the treatment condition.

Images were divided in two parts in ImageJ to separate the CFP channel from the YFP channel. Stacks were realigned to correct for artifactual lateral movement. Data were then analyzed on Matlab by calculating the FRET ratio at each time point for one or several Regions Of Interest (ROIs). The user defined ROIs for each position. For each image, the value of the FRET ratio corresponds to  $\frac{IC-BC}{IY-BY}$  for <sup>T</sup>Epac<sup>vv</sup> probe and to  $\frac{IY-BY}{IC-BC}$  for AKAR4-Kras probe

IY: Mean Intensity of ROI in YFP channel;  
 BY: Mean Intensity of the background in YFP channel;  
 IC: Mean Intensity of ROI in CFP channel;  
 BC: Mean intensity of the background in CFP channel

For each ROI, the FRET ratio was then normalized by the baseline mean, defined as the 7 time points before first treatment application.

$$\text{FRET Ratio normalized to baseline} = 100 * \frac{R_c - R_o}{R_o}$$

Rc: Value of raw FRET ratio

Ro: Mean of the baseline

The quantitative results obtained for each neuronal compartment were grouped together and, for each time point, the mean FRET ratio normalized to baseline and S.E.M. were calculated. Due to CFP photobleaching, FRET ratio tends to increase slowly during the acquisition. This deviation was corrected for somata and dendrites on Matlab. Mean slope was calculated for all neurons in somata and dendrites, respectively, for the last 7 time points before addition of treatment and subtracted from all FRET ratio time points. In the axon, precise execution of this correction is not possible. Indeed, as the signal-to-noise ratio is lower in the extremely thin axons as compared to somata and dendrites, the bleaching is “hidden” in the noise, hindering the precise establishment of the correction slope. Thus, we did not correct for CFP photobleaching in the axon.

#### FRET STATISTICAL ANALYSIS

FRET Response was obtained by calculating the mean FRET ratio in Matlab for 6 time points after treatment, from +4 to +14 min (Response).

Groups were compared using GraphPad Prism. Significance of differences between various conditions was calculated using unpaired *t*-tests or one-way ANOVA with Newman-Keuls post-tests for computing *p* estimates. NS  $p > 0.05$ , \* $p < 0.05$ , \*\* $p < 0.01$  and \*\*\* $p < 0.001$ .

#### IMMUNOCYTOCHEMISTRY

DIV9 hippocampal cultured neurons were briefly rinsed with Dulbecco's PBS (DPBS; PAA laboratories) and fixed in DPBS containing 4% paraformaldehyde and 4% sucrose. After permeabilization with a 5 min incubation in DPBS containing 0.1% Triton X-100 and blocking for 30 min in antibody buffer (DPBS supplemented with 2% BSA and 3% normal goat serum), neurons were incubated with primary antibodies diluted 1:200 (DAGL $\alpha$ ) or 1:250 (MAP2 and Tau) in antibody buffer for 1 h at room temperature. After DPBS rinses, neurons were labeled with secondary antibodies 1:400 in antibody buffer for 30 min at room temperature. Coverslips were fixed with Mowiol containing Hoechst. Images were obtained using a dry 40 $\times$  objective lens on Zeiss Axio Imager M1. Excitation wavelengths of 488 nm (DAGL $\alpha$ ) and 568 nm (MAP2 or Tau) were used.

#### CONFOCAL MICROSCOPY

Hippocampal cultured neurons were cotransfected at DIV6 with DsRed2 and various FRET probes (T<sub>1</sub>Epac<sup>vv</sup>, AKAR4, AKAR4-Kras, Lyn-AKAR4) and fixed in DPBS containing 4% paraformaldehyde and 4% sucrose at DIV7. Images were obtained using an oil immersion objective lens (Plan-Apochromat 60X, NA

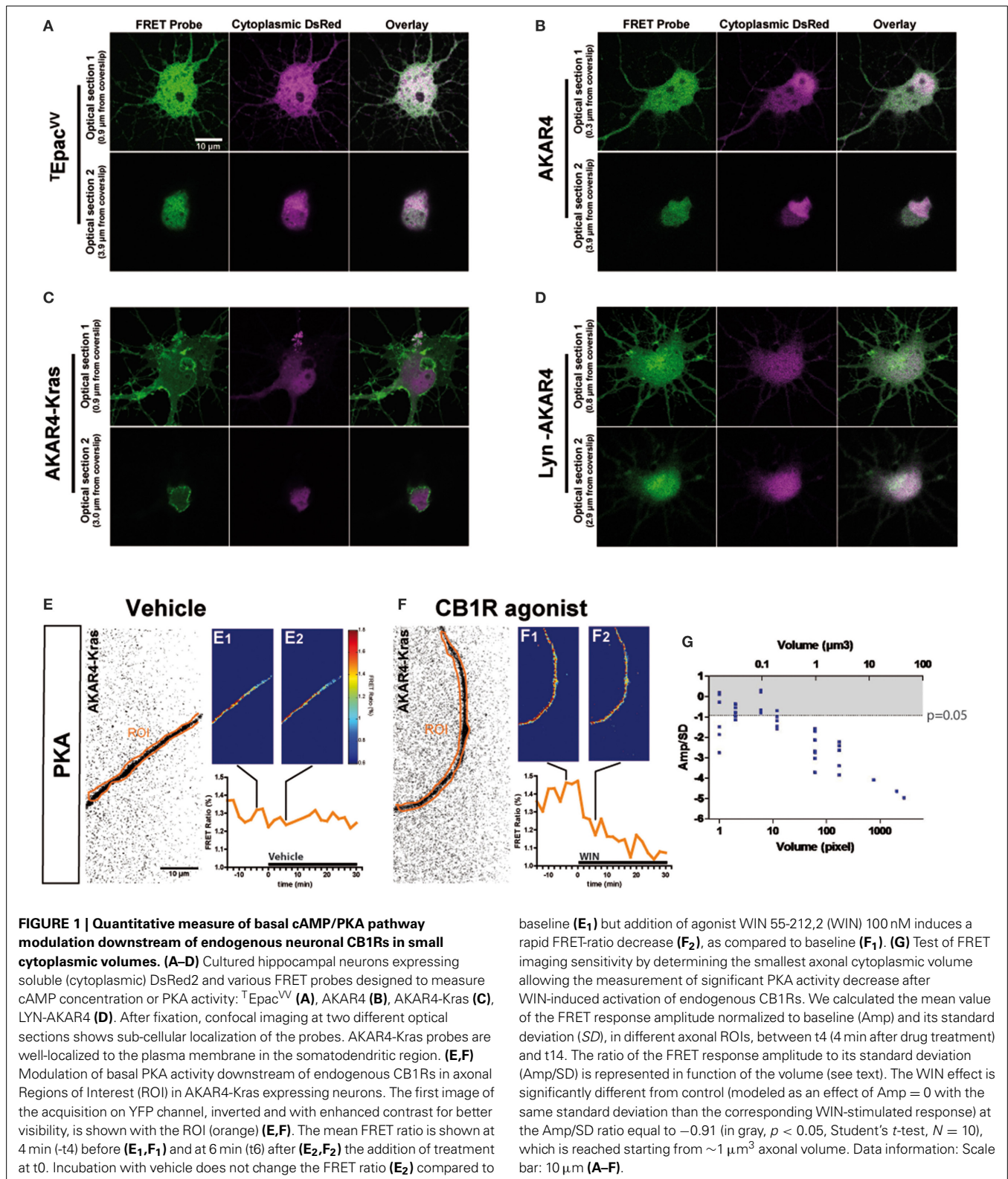
1.4) on a Nikon A1 confocal microscope. Excitation wavelengths of 488 nm (FRET probes) and 568 nm (DsRed2) were used. Stacks were obtained with one image per optical section and 300 nm between each section.

## RESULTS

### ENDOGENOUS CB1Rs MODULATE BASAL PKA ACTIVATION LEVELS IN NEURONS

The characteristic inhibition of cyclic AMP production and PKA activity by G<sub>i/o</sub>-protein coupled GPCRs is usually detected in pharmacological assays after GPCR over-expression and forskolin-induced artificial activation of adenylyl cyclases. Here we aimed to directly measure cannabinoid-induced changes in basal levels of neuronal PKA signaling, downstream of endogenous CB1Rs in cultured hippocampal neurons. Pilot experiments indicated that by using a sensitive EM-CCD camera and hardware-based focus stabilization (see Materials and Methods) we are able to measure cannabinoid-induced inhibition of cyclic AMP production and PKA activity in relatively large cytoplasmic volumes such as neuronal somata by using the soluble T<sub>1</sub>Epac<sup>vv</sup> probe (Klarenbeek et al., 2011) (Figure 1A) and AKAR4 (Depry et al., 2011) (Figure 1B), respectively. However, smaller diameter neurites such as distal dendrites and axons gave weak (low amplitude) and highly variable responses, leading to a low signal-to-noise ratio, which impeded the reliable measure of the relatively small amplitude cannabinoid-induced changes in the FRET ratio with the AKAR4 probe. To overcome this experimental limitation, we hypothesized that, since the PKA activator cAMP is produced by membrane-bound adenylyl cyclases at the plasma membrane and PKA deactivator phosphodiesterases are cytosolic (Neves et al., 2008), targeting a PKA probe to the plasma membrane may strongly increase experimental sensitivity. Indeed, results of a previous report show both higher FRET responses and higher PKA-sensitive potassium current responses downstream of G<sub>s</sub>-protein activation in dendrites that have a high surface-to-volume ratio as compared to the soma (Castro et al., 2010). Therefore, we expressed separately two membrane-targeted PKA biosensors: AKAR4-Kras (Depry et al., 2011), which is targeted to the non-raft domains of the plasma membrane (Figure 1C), and Lyn-AKAR4 (Depry et al., 2011), which is targeted to the raft regions of the plasma membrane (Figure 1D) in well-differentiated hippocampal neurons. In our experimental conditions, AKAR4-Kras showed a more homogenous distribution that segregated well with the plasma membrane at different optical sections of the somatodendritic domain, while Lyn-AKAR4 was more strongly localized to relatively small membrane microdomains and intracellular structures (Figures 1C,D). In order to focus on plasma-membrane localized endogenous CB1Rs, further experiments were therefore performed using AKAR4-Kras.

Does the membrane-targeted AKAR4-Kras probe permit the measurement of cannabinoid-induced modulation of basal PKA levels downstream of endogenous CB1Rs in all neuronal sub-compartments? We tested the sensitivity of our experimental setup by determining the minimal amount of cytoplasmic volume necessary to the detection of cannabinoid-induced modulation of basal PKA levels, in individual thin (mean diameter =



$0.7 \mu\text{m}$ , see Figure 3C) and mature (day *in vitro* 9—DIV9) axons of AKAR4-Kras expressing neurons. By using a large region of interest (ROI) to measure the FRET ratio change, treatment with the synthetic CB1R agonist, WIN55,212-2 (WIN) at

100 nM (Figure 1F), but not with vehicle (Figure 1E), induced a important change of the FRET ratio within 2 min, indicating that CB1R activation induces a decrease of basal PKA activity downstream of endogenous CB1Rs. Measuring the FRET

responses in a single axon by gradually decreasing the size of the ROI, we determined the minimum cytoplasmic volume necessary for reliable measurement of the WIN-induced FRET signal change. ROI volumes have been determined as described in “Supplementary Materials and Methods.” We found that a significant decrease of WIN-induced basal PKA activity downstream of endogenous CB1Rs could be measured in volumes as small as  $1 \mu\text{m}^3$ , which corresponds to 1 femtoliter of axonal cytoplasm (**Figure 1G**), by using a membrane targeted biosensor, such as AKAR4-Kras, possibly because of the high surface-to-volume ratio of extremely thin neurites.

In conclusion, this experimental approach enables the measurement of modulation of basal neuronal PKA activation levels, downstream of an endogenous  $G_{i/o}$  protein coupled receptor, in extremely small cellular volumes, such as the cytoplasm of mature axons.

### TRANSIENT SOMATODENDRITIC CB1RS CONSTITUTIVELY INHIBIT THE cAMP/PKA PATHWAY

Previous ultrastructural analysis of hippocampal neurons has shown that in the somatodendritic region, the steady-state presence of endogenous CB1Rs at the plasma membrane is very low both *in vitro* (Letierrier et al., 2006) and *in vivo* (Katona et al., 1999; Thibault et al., 2013). However, previous studies have also reported that most axonally targeted CB1Rs accomplish a transient passage on the somatodendritic plasma membrane (Letierrier et al., 2006; McDonald et al., 2007; Simon et al., 2013). Currently, it remains unknown whether somatodendritic CB1Rs are able to inhibit cAMP/PKA signaling in this neuronal compartment. Therefore, we measured modulation of basal somatodendritic PKA activity downstream of endogenous CB1Rs and found that treatment with WIN at 100 nM, but not with vehicle, induced a moderate decrease of the FRET ratio in individual neurons within a few minutes (**Figures 2A,B**). To precisely analyze this WIN-induced response, we compared PKA activity in two groups of neurons treated either with vehicle or WIN (100 nM) during 30 min, followed by treatment with the adenylyl cyclase activator Forskolin (Fsk,  $10 \mu\text{M}$ ) (**Figures 2C,D**), to induce a saturating level of AKAR phosphorylation, as reported previously (Gervasi et al., 2007). Fsk induced strong somatodendritic PKA activation with a raw baseline-normalized FRET-ratio increase between 20 and 30%. This increase is in the expected range, since activation of AKAR4-Kras in HEK293 cells by addition of  $50 \mu\text{M}$  Fsk induced an increase of 8% of the raw FRET Ratio (Depry et al., 2011). Conversely, activation of CB1Rs with WIN induced a rapid decrease of basal PKA activity in somata ( $-2.5 \pm 0.4\%$ ) and dendrites ( $-3.2 \pm 0.5\%$ ), which was significant as compared to vehicle (somata:  $0.1 \pm 0.3\%$ , dendrites:  $-0.2 \pm 0.4\%$ ) (**Figures 2C<sub>1</sub>,C<sub>2</sub>,D<sub>1</sub>,D<sub>2</sub>**). Please note that the measured 2–4% changes of the raw baseline-normalized FRET ratio correspond to 10–20% of the maximal response, which equals typically to 20–25% elevation of the raw baseline-normalized FRET ratio, as established by the terminal saturating Fsk treatment. Given that endogenous CB1Rs are not the only  $G_{\alpha_{i/o}}$ -coupled GPCRs in hippocampal neurons, mobilization of the cAMP/PKA pathway in the 10–20% range of the maximal response suggests physiological relevance. Moreover, FRET responses showed

Gaussian distribution pattern (as verified by the normality test), indicating that hippocampal neurons did not segregate into subpopulations regarding the effects of CB1R agonist/antagonist application (Supplementary Figures 1A–C). This is in contrast to a previous *ex-vivo* report that studied somatic slow self-inhibition in cortical neurons, where only a subpopulation of neurons was responsive to cannabinoid treatment (Marinelli et al., 2009). The effect of WIN was blocked after overnight treatment with 100 ng/mL of the  $G_{i/o}$ -protein specific inhibitor pertussis toxin (PTX) (somata:  $-0.3 \pm 0.2\%$ , dendrites:  $-1.5 \pm 0.3\%$ ) as well as after 3 h pre-treatment with  $1 \mu\text{M}$  of the CB1R-specific antagonist/inverse-agonist AM281 (somata:  $0.3 \pm 0.3\%$ , dendrites:  $-1.1 \pm 0.5\%$ ). Therefore, endogenous CB1Rs, transiently present on the somatodendritic plasma membrane, can be activated by exogenous cannabinoids and are able to subsequently inhibit basal PKA signaling through their coupling to  $G_{i/o}$  proteins both in somata and dendrites.

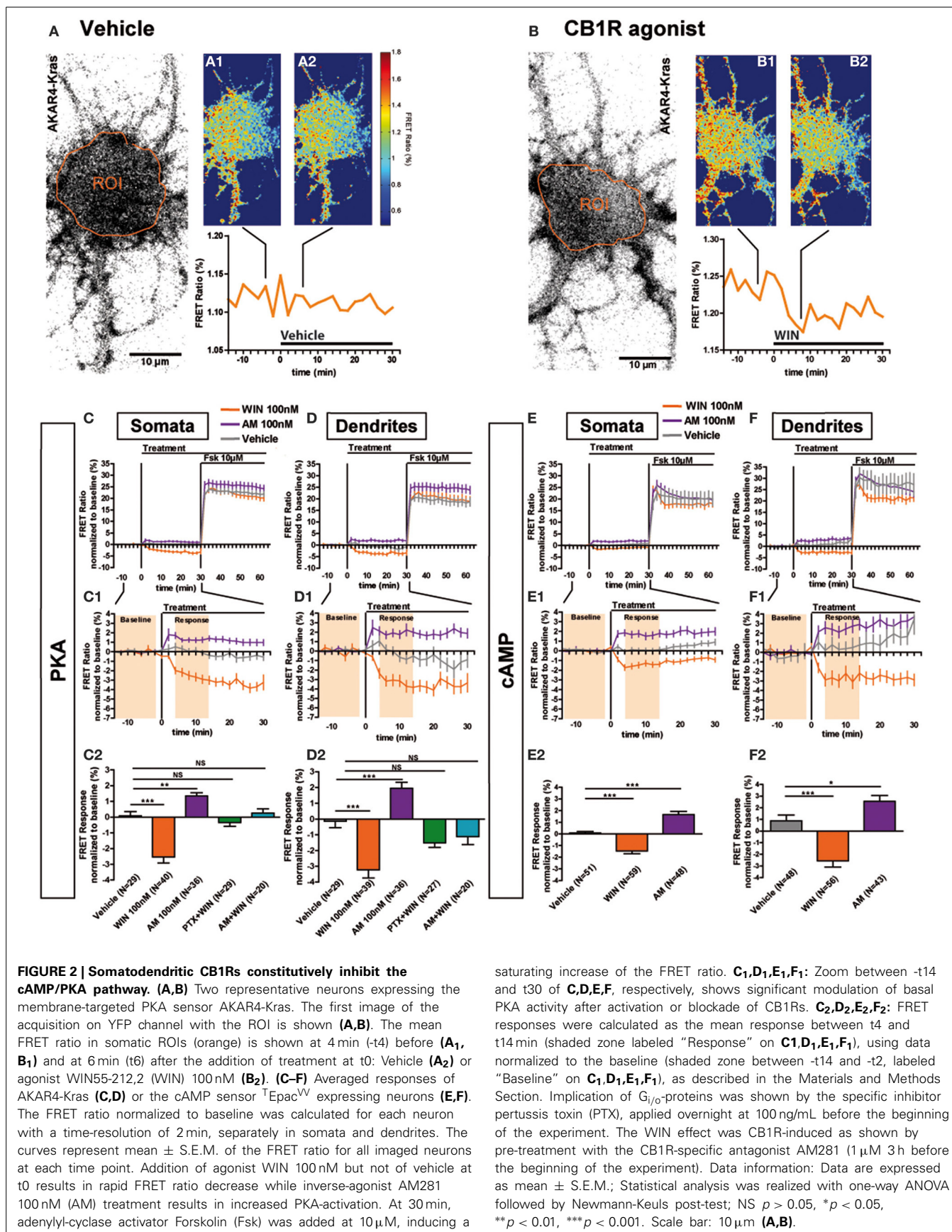
We have previously reported that somatodendritic CB1Rs are constitutively endocytosed because of constitutive receptor activation, which can be inhibited by pharmacological or genetic tools (Letierrier et al., 2006; Simon et al., 2013). To investigate whether CB1Rs also constitutively inhibit cAMP/PKA signaling in the somatodendritic compartment, we applied the CB1R inverse agonist, AM281 at 100 nM, to neurons expressing AKAR4-Kras. This treatment led to a rapid and significant increase of the FRET ratio both in somata and dendrites (somata:  $1.3 \pm 0.2\%$ , dendrites:  $2.0 \pm 0.4\%$ ) (**Figures 2C<sub>1</sub>,C<sub>2</sub>,D<sub>1</sub>,D<sub>2</sub>**). Therefore, somatodendritic CB1Rs exert a constitutive inhibition on PKA activity that is removed by inverse agonist treatment.

Taken together these results indicate that somatodendritic CB1Rs constitutively inhibit PKA activity through the mobilization of  $G_{i/o}$  proteins, which is likely due to the inhibition of adenylyl cyclase and subsequent decrease of cAMP production. To confirm this mechanism, we directly measured the modulation of basal somatodendritic cAMP concentration, downstream of CB1Rs, by using the  $^T\text{Epac}^{\text{VV}}$  probe (Klarenbeek et al., 2011). The activation of endogenous CB1Rs with WIN (100 nM) induced a rapid and significant decrease of cAMP concentration in somata ( $-1.5 \pm 0.3\%$ ) and dendrites ( $-2.6 \pm 0.6\%$ ), while application of the inverse agonist AM281 at 100 nM led to a rapid and significant increase of cAMP concentration both in somata ( $1.7 \pm 0.3\%$ ) and dendrites ( $2.6 \pm 0.5\%$ ) (**Figures 2E,E<sub>1</sub>,E<sub>2</sub>,F,F<sub>1</sub>,F<sub>2</sub>**). Responses to the final  $10 \mu\text{M}$  Fsk treatment are also a slightly different. However, accurate measure of ligand-induced modifications of artificial adenylyl cyclase stimulation by Fsk was not the scope of the present study, where we focused on endogenous CB1R-induced modification of basal PKA activation levels.

These results show that endogenous CB1Rs exert a constitutive inhibition on the cAMP/PKA signaling pathway both in somata and dendrites. In addition, somatodendritic CB1Rs can be further activated by exogenous cannabinoids leading to a rapid decrease of cAMP concentration and PKA activity through activation of  $G_{i/o}$  proteins.

### AXONAL CB1R SIGNALING IS DIFFERENT FROM DENDRITIC SIGNALING

Previous studies have found a polarized accumulation of transcytosed CB1Rs on the axonal plasma membrane due to reduced



internalization levels as compared to dendrites (Leterrier et al., 2006; McDonald et al., 2007; Simon et al., 2013). We asked whether the recruitment of signaling pathways downstream of CB1Rs in axons also differ from somata and dendrites. Application of 100 nM WIN led to a rapid and significant decrease of basal PKA activity in axons ( $-14.6 \pm 1.4\%$ ) compared to vehicle ( $-1.8 \pm 0.6\%$ ) (Figures 3A,A<sub>1</sub>,A<sub>2</sub>). This effect was blocked by pre-treatment with AM281 1  $\mu\text{M}$  ( $-2.6 \pm 1.0\%$ ) and PTX 100 ng/mL ( $-5.5 \pm 1.1\%$ ), showing that PKA inhibition is specifically mediated by CB1Rs acting through G<sub>i/o</sub> proteins. In addition, CB1R activation decreased PKA activity more strongly in the axon than in dendrites (dendrite response normalized to vehicle:  $-3.1 \pm 0.5\%$ , axonal response normalized to vehicle:  $-12.8 \pm 1.4$ ) (Figure 3B). Interestingly, in contrast to dendrites, application of the inverse agonist AM281 at 100 nM did not induce a detectable change of PKA activity in the axon ( $0.1 \pm 0.8\%$ ), suggesting that axonal CB1Rs are not constitutively activated (Figures 3A,A<sub>1</sub>,A<sub>2</sub>).

Why does axonal CB1R activation lead to a significantly higher amplitude of PKA inhibition in axons than in dendrites and somata? First, similarly to their distribution *in vivo* (Katona et al., 2001; Bodor et al., 2005; Thibault et al., 2013), CB1Rs display an axonally polarized distribution in cultured neurons (Coutts et al., 2001; Leterrier et al., 2006; McDonald et al., 2007; Simon et al., 2013). Second, theoretical models predict, and experiments show that, for signaling molecules produced at the plasma membrane and degraded in the cytoplasm, such as cAMP, the ratio of the surface area of the plasma membrane to the cytoplasmic volume [surface/volume ratio (S/V)] becomes important (Neves et al., 2008). As such, we asked whether the strong decrease of PKA activity observed after CB1R activation in the axon is related to the high S/V ratio of this compartment. However, for both axons and distal dendrites, we found no correlation between neurite diameter and FRET response amplitude after CB1R activation (Pearson's correlation coefficient:  $r_{\text{distal dendrites}} = -0.065$  and  $r_{\text{axons}} = 0.03649$ ) (Figure 3C). Moreover, a sub-population of distal dendrites has the same diameter range as axons. In these thin dendritic segments, the amplitude of the FRET response after CB1R activation was again significantly different from the axonal response (dendrites normalized to vehicle:  $-4.0 \pm 0.8\%$ , axons normalized to vehicle:  $-12.8 \pm 1.4$ ) (Figure 3D). Therefore, morphological differences between axons and dendrites do not explain the observed signaling disparity among these two compartments, suggesting that the polarized distribution of neuronal CB1Rs is the main reason for the enhanced agonist response in axons.

#### CONSTITUTIVE ACTIVATION OF SOMATODENDRITIC CB1RS REQUIRES LOCAL SYNTHESIS OF ENDOCANNABINOIDS

Next we investigated why CB1Rs are constitutively activated in the somatodendritic compartment but not in the axon, by focusing on the contribution of endocannabinoids, which play an important role in basal CB1R activation in several experimental systems (Turu et al., 2007; Howlett et al., 2011). The major endocannabinoid 2-arachidonoylglycerol (2-AG) is a lipid molecule present in the cell plasma membrane and is synthesized by DAG Lipases (DAGL). DAGL $\alpha$ , the major DAGL in the postnatal brain,

is segregated to axonal tracts during embryonic development but was shown to accumulate after birth in the somatodendritic plasma membrane in several brain areas, such as the cerebellum (Bisogno et al., 2003), striatum (Uchigashima et al., 2007), hippocampus (Katona et al., 2006; Yoshida et al., 2006) and amygdala (Yoshida et al., 2011). Similarly, we found a somatodendritic segregation of DAGL $\alpha$  in fully-polarized (DIV9) cultured hippocampal neurons, while no labeling was found in the axon (Figures 4A,A<sub>1</sub>). This indicates local production of 2-AG in the plasma membrane of the somatodendritic compartment but not in the axonal counterpart. To investigate whether such polarized 2-AG production may explain the aforementioned differences in constitutive CB1R activation between dendrites and axons, we pre-treated neurons expressing the AKAR4-Kras probe with the DAGL inhibitors, Tetrahydrolipstatin (THL) or RHC80267 (RHC), during 3 h before treatment with the inverse agonist AM281 100 nM (Figures 4B,B<sub>1</sub>,C,C<sub>1</sub>). The FRET ratio did not increase in these neurons after adding AM281, neither in somata (AM281:  $1.6 \pm 0.3\%$ , vehicle:  $0.2 \pm 0.3\%$ , AM281 after THL 1  $\mu\text{M}$ :  $0.4 \pm 0.3\%$ , AM281 after RHC 25  $\mu\text{M}$ :  $0.1 \pm 0.3\%$ ) nor in dendrites (AM281:  $2.0 \pm 0.5\%$ , vehicle:  $0.4 \pm 0.4\%$ , AM281 after THL 1  $\mu\text{M}$ :  $0.4 \pm 0.3\%$ , AM281 after RHC 25  $\mu\text{M}$ :  $-0.1 \pm 0.5\%$ ). Thus, the constitutive inhibition on PKA activity was removed by DAGL blockade, demonstrating that constitutive activation of somatodendritic CB1Rs requires locally produced 2-AG.

#### SIGNALING RESPONSES TO EXOGENOUS LIGANDS WIN, CP55,940 AND $\Delta^9$ -THC ARE DIFFERENTIALLY SHAPED BY LOCAL PRODUCTION OF 2-AG IN THE SOMATODENDRITIC COMPARTMENT

Previous results show that, after DAGL inhibition, the amount of CB1Rs increase on the plasma membrane, both in the somatodendritic compartments of neurons and in CHO cells (Turu et al., 2007). In CHO cells, the elevated CB1R levels at the plasma membrane yield enhanced G-protein activation following WIN administration (Turu et al., 2007). We asked whether the THL-induced accumulation of CB1Rs on the somatodendritic membrane is able to produce similar enhanced inhibition of PKA activity after WIN administration, as compared to basal conditions. Therefore, we pre-treated neurons with THL (1  $\mu\text{M}$ ) during 3 h before acquisition and applied WIN during the FRET acquisition (Figure 5A). Surprisingly, DAGL inhibition blocked the effect of 100 nM WIN in the somatodendritic compartment instead of signaling enhancement (somatic response to WIN 100nM:  $-2.4 \pm 0.4\%$ ,  $P < 0.01$  compared to vehicle ( $0.1 \pm 0.2\%$ ) and  $P < 0.01$  compared to response to WIN 100 nM after 3 h THL 1  $\mu\text{M}$  ( $-0.2 \pm 0.6\%$ ), one-way ANOVA followed by Newman-Keuls post-test; dendrite response to WIN 100 nM:  $-2.8 \pm 0.4\%$ ,  $P < 0.01$  compared to vehicle ( $-0.4 \pm 0.4\%$ ) and  $P < 0.01$  compared to response to WIN 100 nM after 3 h THL 1  $\mu\text{M}$  ( $-0.6 \pm 0.6\%$ ), one-way ANOVA followed by Newman-Keuls post-test) (Figures 5A,A<sub>1</sub>,C,C<sub>1</sub>), while it did not change the FRET response in the axon (response to WIN 100 nM:  $-14.6 \pm 1.1\%$ ,  $P < 0.001$  compared to vehicle ( $-1.9 \pm 0.9\%$ ) and  $P > 0.05$  compared to WIN 100 nM after 3 h THL 1  $\mu\text{M}$  ( $-12.4 \pm 1.2\%$ ), one-way ANOVA followed by Newman-Keuls post-test) (Figures 5A<sub>2</sub>,C<sub>2</sub>). This suggests that a local 2-AG production drop, caused by THL pre-treatment, was

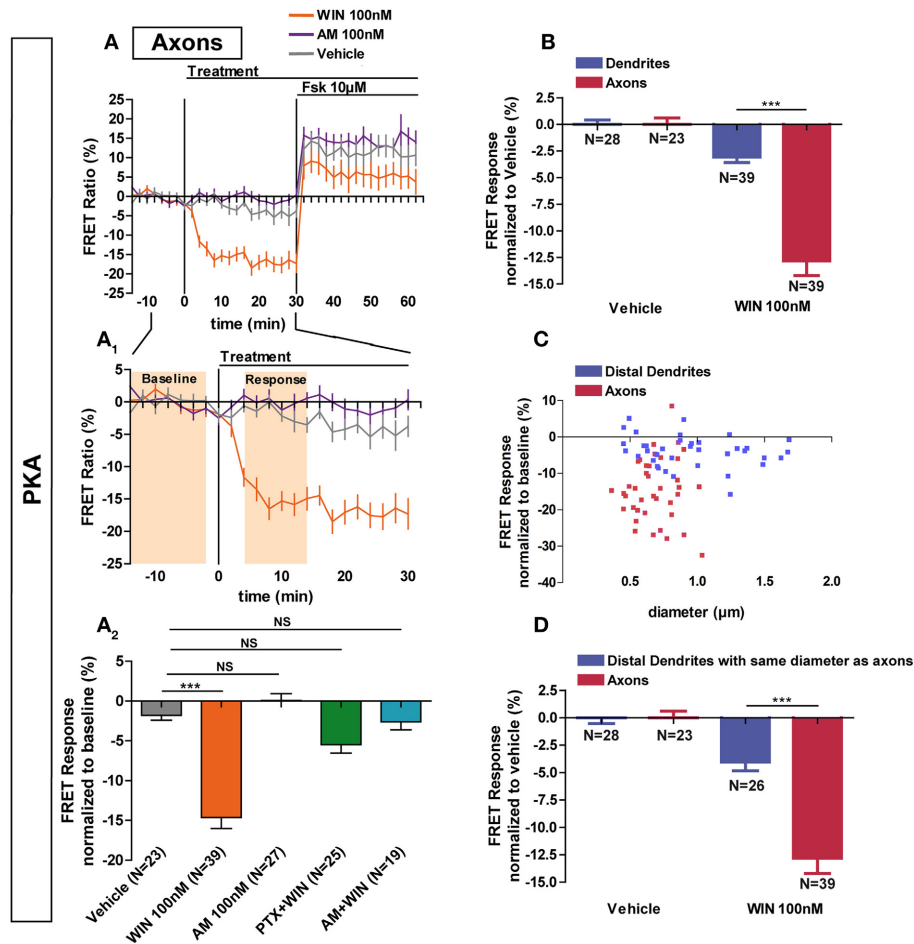


**FIGURE 3 | Axonal CB1R signaling differs from dendritic signaling. (A)**

Averaged axonal responses of AKAR4-Kras expressing neurons, as shown on **Figures 1E,F**. The FRET ratio normalized to baseline was calculated for each neuron with a time-resolution of 2 min. The curves represent mean  $\pm$  S.E.M. of the FRET ratio for all imaged neurons at each time point. Addition of agonist WIN 100 nM but not of vehicle or inverse-agonist AM281 100 nM (AM) at t0 results in rapid high-amplitude FRET ratio decrease. At 30 min, adenylyl-cyclase activator Forskolin (Fsk) was added at 10  $\mu$ M, inducing a saturating increase of the FRET ratio. **A1**: Zoom between -t14 and t30 of **A** shows significant modulation of basal PKA activity after activation of CB1Rs. **A2**: FRET responses were calculated as the mean response between t4 and t14 min (shaded zone labeled "Response" on **A1**), using data normalized to the baseline (shaded zone between -t14 and -t2, labeled "Baseline" on **A1**). Implication of G<sub>1/0</sub>-proteins was shown by the specific inhibitor pertussis

toxin (PTX), applied overnight at 100 ng/mL before the beginning of the experiment. The WIN effect was CB1R-induced as shown by pre-treatment with the CB1R-specific antagonist AM281 (1  $\mu$ M, 3 h before the beginning of the experiment). **(B)** Vehicle-normalized FRET response to WIN is significantly stronger in axons than in dendrites. **(C)** Individual FRET responses in axons and distal dendrites are represented in function of their respective diameter. For each group (distal dendrites and axons), a Pearson correlation test was calculated showing no correlation between FRET response and diameter ( $r_{\text{distal dendrites}} = -0.065$  and  $r_{\text{axons}} = 0.03649$ ). **(D)** Distal dendrites having the similar diameter than axons still display significantly weaker vehicle-normalized FRET responses to WIN compared to axons. Data information: Data are expressed as means  $\pm$  S.E.M.; Statistical analysis was realized with one-way ANOVA followed by Newmann-Keuls post-test (**A2**) or unpaired t-test (**B,D**); NS  $p > 0.05$ , \*\*\* $p < 0.001$ .

responsible for the somatodendritic signaling decrease, which indeed could be rescued by 2-AG (100 nM), applied for 10 min before WIN treatment (somata:  $-3.3 \pm 1.0\%$ , dendrites:  $-3.7 \pm 1.2\%$ , axons:  $-11.8 \pm 1.6\%$ ; WIN responses were compared to vehicle) (**Figures 5B,B1,C,C1,C2**). By itself, 2-AG used at 1  $\mu$ M is able to decrease PKA activity in all neuronal compartments, with a stronger effect in axons as compared to the somatodendritic compartment (somata:  $-2.6 \pm 0.7\%$ , dendrites:  $-5.5 \pm 0.5\%$ , axons:  $-17.7 \pm 1.5\%$ ) (**Figures 5C,C1,C2**). To verify if the presence of local 2-AG is a general requirement for somatodendritic CB1R activation, we tested two other, structurally

different, CB1R agonists: CP55,940 (CP) and  $\Delta^9$ -THC (THC), the psychoactive compound of marijuana. In control neurons, the effect of CB1R activation with 100 nM CP was comparable to WIN, with a decrease of PKA activity in both dendrites and axons as well as a stronger amplitude in the axonal response compared to dendrites (somata:  $-1.0 \pm 0.4\%$ ; dendrites:  $-2.1 \pm 0.7\%$ ; axons:  $-18.4 \pm 1.6\%$ ) (**Figures 5C,C1,C2**). However, blockade of DAGL by THL pretreatment did not decrease the effect of CP (100 nM) in the somatodendritic compartment. On the contrary, and according to our previous expectations for WIN, this response was enhanced as compared to control neurons

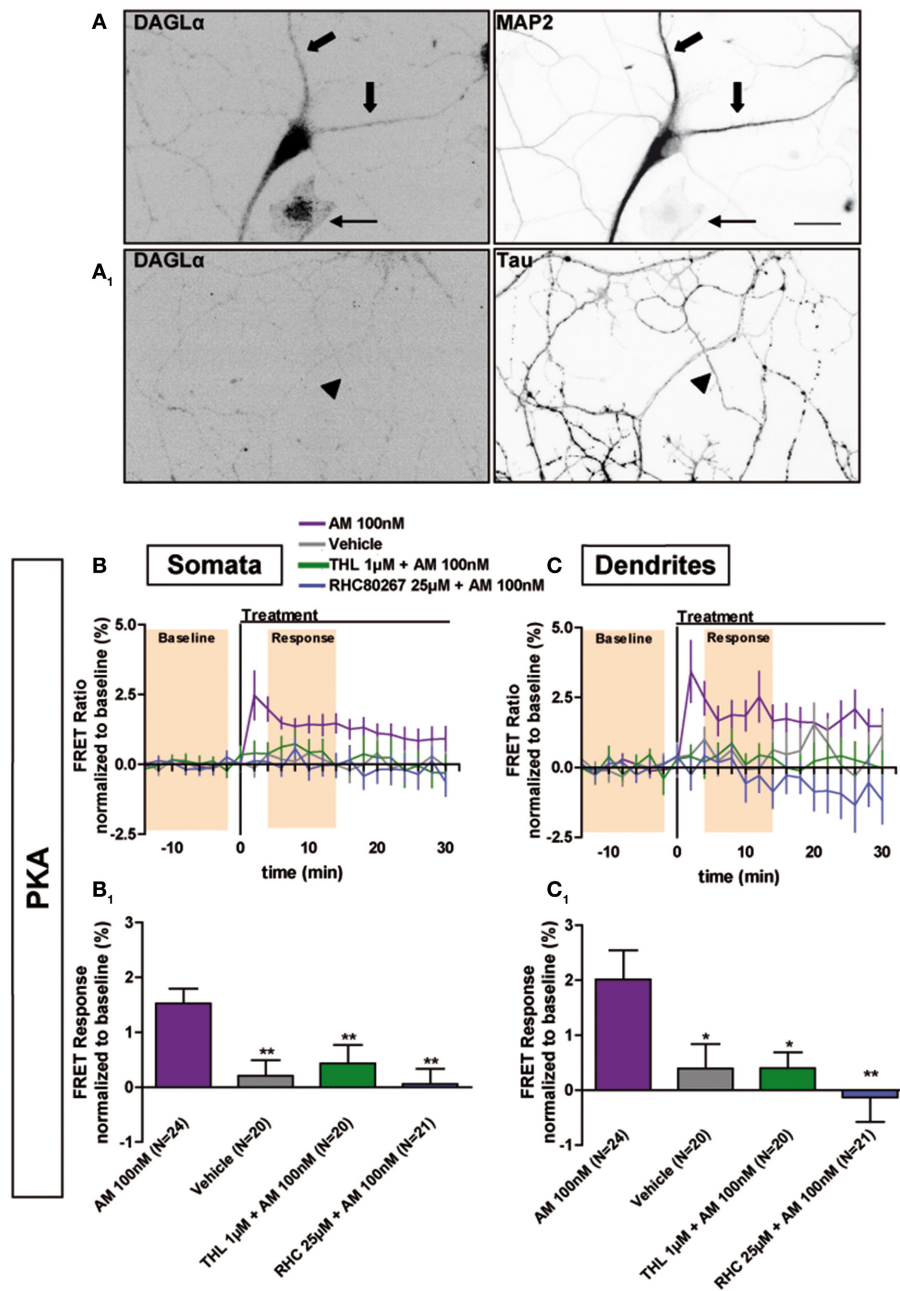


**FIGURE 4 | Constitutive activation of somatodendritic CB1Rs requires locally synthesized endocannabinoids.** (A) Simultaneous immunolabeling of fully-polarized (DIV9) neurons with anti-DAGL $\alpha$  antibody and either anti-MAP2 (A) or anti-Tau (A<sub>1</sub>) antibodies. Large arrows indicate dendrites, arrow-heads indicate axon and the thin arrow shows an astrocyte. (B,C) Averaged somatic and dendritic responses of AKAR4-Kras expressing neurons to inverse-agonist AM281 (AM), with or without inhibiting DAGL activity. The FRET ratio normalized to baseline was calculated for each neuron

with a time-resolution of 2 min. The curves represent mean  $\pm$  S.E.M. of the FRET ratio for all imaged neurons at each time point. Addition of 100 nM AM but not of vehicle at t<sub>0</sub> results in elevated PKA activity, revealing constitutive CB1R activation, which is significantly decreased after DAGL inhibition either by tetrahydrolipstatin (THL) 1  $\mu$ M or RHC80267 25  $\mu$ M. Data information: Data are expressed as mean  $\pm$  S.E.M.; Statistical analysis was realized with one-way ANOVA followed by Newmann-Keuls post-test; \* $p$  < 0.05, \*\* $p$  < 0.01. Scale bar: 20  $\mu$ m (A,A<sub>1</sub>).

(somata:  $-5.0 \pm 1.2\%$ , dendrites:  $-5.7 \pm 1.3\%$ , axons:  $-19.2 \pm 1.4\%$ ; responses to CP 100 nM after 3 h THL 1  $\mu$ M were compared to CP 100 nM alone). Finally, treatment with THC (1  $\mu$ M) also decreased PKA activity in all neuronal compartments, with a stronger effect in the axon compared to the somatodendritic compartment (somata:  $-1.5 \pm 0.4\%$ , dendrites:  $-2.8 \pm 0.5\%$ ,

axons:  $-15.8 \pm 2.1\%$ ) (Figures 5C,C<sub>1</sub>,C<sub>2</sub>). However, the somatodendritic effect of 1  $\mu$ M THC was suppressed by THL pre-treatment while it did not affect the axonal response (somata:  $-0.3 \pm 0.7\%$ , dendrites:  $0.1 \pm 1.0\%$ , axons:  $-14.2 \pm 2.5\%$ ; responses to THC 1  $\mu$ M after 3 h THL 1  $\mu$ M were compared to THC 1  $\mu$ M alone) (Figures 5C,C<sub>1</sub>,C<sub>2</sub>). Thus, THC and WIN

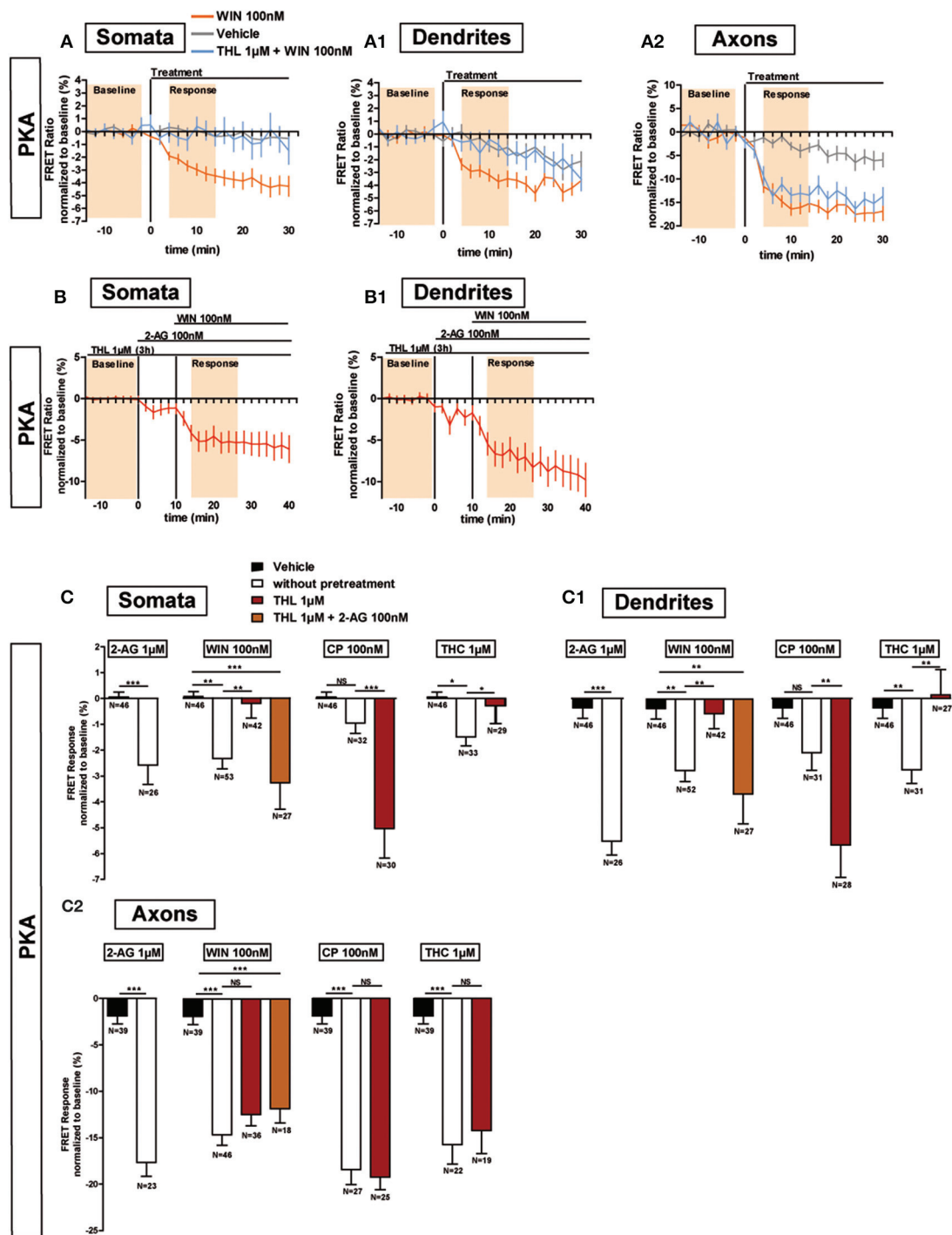


**FIGURE 5 | Endogenous 2-AG significantly modifies CB1R responses to exogenous cannabinoids. (A,B)** Averaged somatic, dendritic and axonal responses of AKAR4-Kras expressing neurons to agonist WIN 55-212,2 (WIN). The FRET ratio normalized to baseline was calculated for each neuron with a time-resolution of 2 min. The curves represent mean  $\pm$  S.E.M. of the FRET ratio for all imaged neurons at each time point. Addition of WIN 100 nM but not of vehicle at t0 results in decreased PKA activity, which effect is significantly inhibited after DAGL inhibition by tetrahydrolipstatin (THL) 1  $\mu$ M in somata (**A**) and dendrites (**A1**) but not in axons (**A2**). The effect of THL pre-treatment on the WIN effect in somata (**B**) and dendrites (**B1**) can be rescued by applying 2-AG at 100 nM 10 min before WIN. (**C**) Variation of

neuronal 2-AG levels (similarly to **A,B**) modifies the FRET responses to exocannabinoids WIN55-212,2 100 nM (WIN), CP55,940 100 nM (CP) and  $\Delta^9$ -THC 1  $\mu$ M (THC), shown as the mean response between t4 and t14 min (shaded zone labeled "Response" on **A,B**), using data normalized to the baseline (shaded zone between -t14 and -t2, labeled "Baseline" on **A,B**) in somata (**C**), dendrites (**C1**) or axons (**C2**). 2-AG levels were reduced by THL 1  $\mu$ M, applied 3 h before the beginning of the experiment and rescued by 2-AG 100 nM at 10 min before agonist treatment. Data information: Data are expressed as mean  $\pm$  S.E.M.; Statistical analysis was realized with unpaired *t*-test (2-AG) or one-way ANOVA followed by Newmann-Keuls post-test (WIN, CP, and THC); NS  $p > 0.05$ , \* $p < 0.05$ , \*\* $p < 0.01$  and \*\*\* $p < 0.001$ .

require local presence of 2-AG to activate somatodendritic CB1Rs.

In conclusion, activation of CB1Rs by exogenous cannabinoids can have contrasted effects on the mobilization of somatodendritic signaling pathways: these effects are highly shaped by local presence of 2-AG which is necessary for the effects of both WIN and THC, but not of CP, in this neuronal compartment.

## DISCUSSION

We developed a highly sensitive quantitative *in vitro* method to evaluate, for the first time to our knowledge, the modulation of the cAMP/PKA signaling pathway downstream of an endogenous  $G_{i/o}$  protein coupled receptor with sub-neuronal resolution. We measured modulation of basal cAMP/PKA signaling, after activation or blockade of endogenous CB1Rs, in somata, dendrites and axons of well-differentiated cultured rat hippocampal neurons. Our results show that polarized distribution of two neuronal proteins, the endocannabinoid synthesizing DAGL $\alpha$  enzyme and the CB1R, leads to previously unappreciated quantitative sub-domain dependent differences in intraneuronal GPCR signaling. In axons, the combined effect of high CB1R density and absence of DAGL $\alpha$  activity leads both to elevated response amplitude following agonist stimulation, as well as to a lack of constitutive activation. In the somatodendritic compartment, relatively low CB1R density and high DAGL $\alpha$  activity, locally producing the membrane component endocannabinoid 2-AG, results in constitutive activation of CB1R-activated signaling which is accompanied by significant but relatively low amplitude agonist-induced signaling responses.

In addition, we show that the 2-AG content of the somatodendritic plasma membrane has contrasted effects on CB1R activation by various exogenous cannabinoid ligands: at the ligand concentrations used in the present study, CP acts as a classical agonist while both WIN and THC require the presence of endogenous 2-AG to efficiently activate CB1Rs.

### CB1RS CONSTITUTIVELY INHIBIT cAMP/PKA SIGNALING IN THE SOMATODENDRITIC COMPARTMENT BUT NOT IN THE AXON

Several studies reported that CB1Rs display constitutive activity in neurons (Pan et al., 1998; Hillard et al., 1999) and notably, these receptors are constitutively endocytosed in the somatodendritic compartment, but not in axons, due to basal activation (Leterrier et al., 2006; Simon et al., 2013). Here we show that application of the inverse agonist AM281 leads to a rapid increase in both somatodendritic cAMP concentration and PKA activity, suggesting constitutive CB1R activation in the somatodendritic compartment but not in the axon. In non-polarized cells, constitutive CB1R activity is highly diminished in the absence of endocannabinoid 2-AG (Turu et al., 2007). We found here that DAGL $\alpha$  is segregated in the somatodendritic compartment and its inhibition removes the effect of AM281. Therefore, somatodendritic CB1Rs are constitutively activated by a high-tone of locally produced 2-AG, and the lack of constitutive activity in the axon is due to the absence of 2-AG.

Our results show important somatodendritic effects on cAMP/PKA regulation for an axonal (i.e., presynaptic) receptor.

Previously, CB1R-mediated somatodendritic slow self-inhibition (SSI) was reported in neocortical interneurons (Bacci et al., 2004) and pyramidal neurons (Marinelli et al., 2009). During SSI, activation-induced post-synaptic increase of calcium stimulates somatodendritic DAGL, leading to local 2-AG production and cell-autonomous activation of somatodendritic CB1Rs and G protein inwardly rectifying  $K^+$  (GIRK) channels (Marinelli et al., 2008). Our results are coherent with these observations and extend the mechanical understanding of the phenomenon.  $\beta\gamma$  subunits of  $G_{i/o}$  proteins may directly activate GIRK channels (Lujan et al., 2009). Here we directly demonstrate that such  $G_{i/o}$  proteins can be activated by CB1Rs in the somatodendritic region and we show that this activation impacts on local cAMP and PKA activation levels. Therefore, it is likely that SSI-inducing activation leads to a parallel decrease of somatodendritic cAMP levels and to PKA inhibition. Interestingly, while cortical neurons are segregated into sub-populations that respond differently to CB1R activation *ex vivo* (Marinelli et al., 2009), our results, which show a Gaussian distribution in responses (Supplementary Figure 1), suggest that either such sub-populations are not present in hippocampal neurons or that our technique is not sensitive enough to detect such differences. We also report that basal production of 2-AG is both necessary and sufficient to activate  $G_{i/o}$  proteins through CB1Rs to achieve measurable constitutive inhibition of somatodendritic cAMP/PKA signaling. GPCRs may also display constitutive activity due to conformational instability (Kenakin, 2004) and several studies reported that CB1Rs may display constitutive activity in systems apparently free of endocannabinoids (review in Pertwee, 2005). However, it is difficult to formally exclude the presence of endocannabinoids, since these lipid molecules may be present in cell plasma membrane at high levels even in non-stimulated neurons (Alger and Kim, 2011).

Here, our results indicate the complete elimination of measurable constitutive somatodendritic CB1R activation after pharmacological inhibition of DAGL and the lack of constitutive activation in the mature axon, where the absence of DAGL suggests low levels of membrane-borne 2-AG. However, a certain level of conformational instability may be necessary to enable constitutive activation of CB1R by 2-AG. Alanine substitution of the T210 residue, which is located in the 3rd transmembrane helix and is well-conserved in the cannabinoid receptor family but absent in other class A GPCRs (D'Antona et al., 2006), results in change of the CB1R conformational state (Simon et al., 2013) and yields a hypoactive receptor form, which displays significantly lower constitutive activity but preserves responsiveness to agonists (D'Antona et al., 2006). Overexpressed T210A mutant CB1Rs accumulate on the somatodendritic surface because of reduced steady-state endocytosis and this accumulation leads to elevated somatodendritic responses to WIN treatment (Simon et al., 2013). To further understand the effect of conformational instability induced by T210 on CB1R signaling, it would be useful in the future to induce the T210A mutation in the endogenous CB1R through a genetic editing approach, in order to avoid the putative effects of receptor overexpression on the signaling response.

### CB1R ACTIVATION BY EXOGENOUS CANNABINOIDS IN AXONS DIFFERS FROM THAT IN DENDRITES, WHERE LOCAL 2-AG MODULATES THE RESPONSE TO AGONISTS

Activation of endogenous CB1Rs leads to a stronger decrease of PKA activity in axons compared to dendrites. This difference is not due to the shape of neurites. CB1Rs are enriched in the axonal plasma membrane, leading to approximately 10-fold more endogenous CB1Rs receptors at the plasma membrane in axons as compared to dendrites (McDonald et al., 2007). Here, we observed that the decrease of PKA activity after CB1R activation is about 3-fold stronger in the axon than in dendrites. Thus, differences in sub-neuronal signaling and receptor density are in the same range, suggesting that the main cause of the polarized signaling response is polarized CB1R distribution. Our previous results have shown that polarized spatial distribution of CB1Rs is precisely regulated by steady-state somatodendritic activation and endocytosis coupled to trans-cytotic targeting (Simon et al., 2013), so it is likely that polarized distribution (i.e., somatodendritic segregation) of DAGL $\alpha$  is the principal cause of the polarized distribution of CB1Rs. However, this model is based on previous data obtained by using a highly-sensitive quantitative experimental approach employing overexpressed epitope-tagged CB1Rs and exogenous cannabinoids (Simon et al., 2013). In future studies, it would be interesting to verify this hypothesis with sensitive detection of endogenous CB1R localization and well-controlled modification of cell-autonomous endocannabinoid levels.

Our results also indicate that inhibition of 2-AG synthesis prevents WIN-induced activation of CB1Rs in the somatodendritic compartment, whereas, in the axon, absence of 2-AG leads to a lack of constitutive activity but does not prevent activation by WIN. Presently, possible interactions between 2-AG and WIN on CB1R activation are not clearly understood. CB1R intramembrane loops were proposed to shape a “binding pocket” that 2-AG could reach through a gap allowing lipidic ligands to enter from membrane bilayer, without need of extracellular access (Hurst et al., 2013). Aminoalkylindole cannabinoids such as WIN bind at a different site (McAllister et al., 2003; Hurst et al., 2013), so WIN could act as a positive allosteric modulator for 2-AG, by increasing 2-AG-induced constitutive CB1R activation, leading to enhanced inhibition of cAMP/PKA signaling in the somatodendritic compartment. Interestingly, the agonist CP55,940 binds at a different site than WIN (Kapur et al., 2007) and dissimilarly to WIN, CP55,940-mediated inhibition of somatodendritic PKA activity is significantly stronger after DAGL inhibition. After DAGL inhibition, CB1R levels increase at the somatodendritic plasma membrane because of reduced endocytic elimination (Turu et al., 2007) possibly explaining the enhanced CP effect in the somatodendritic compartment. In the axon, CP-induced PKA activity decrease is not modified by THL, as DAGL is absent in this compartment. Finally, the phytocannabinoid THC induces a decrease of PKA activity in the somatodendritic compartment that is removed after DAGL inhibition. Therefore, neuronal pharmacology of THC is similar to WIN but not to CP, suggesting that THC may also act as an exogenous positive allosteric modulator, that amplifies the CB1R-activating effect of locally

produced 2-AG in the somatodendritic compartment. These surprising interactions between 2-AG and exogenous cannabinoid ligands may result from changes in CB1R levels on the somatodendritic surface but also from different, potentially overlapping and to date not completely understood mechanisms, such as conformation-induced changes in ligand affinity and efficiency and competition for ligand binding sites. Full comprehension of these effects requires further technical development that, through enhancing the sensitivity of the experimental approach presented here, may allow detailed pharmacological characterization in the future, such as precise measurement of ligand affinity and efficacy, of endogenous GPCR signaling in neuronal sub-domains.

In conclusion, our results show that pharmacological responses to activation of a major neuronal GPCR are different in axons and dendrites. In the somatodendritic compartment, CB1Rs are constitutively activated by locally produced 2-AG, constitutively inhibit the cAMP/PKA pathway and can be further activated, significantly albeit moderately, by exogenous cannabinoids. A similar activation profile was reported in non-polarized cells (Turu et al., 2007). However, the pharmacological profile of axonal CB1Rs is different: their activation leads to a strong decrease of PKA activity and no significant constitutive activation is observed. This highly contrasted difference in sub-neuronal signaling responses warrants caution in extrapolating pharmacological profiles, which are typically obtained in non-polarized cells, to predict *in vivo* responses of axonal (i.e., presynaptic) GPCRs. Therefore, the *in situ* pharmacological approach presented in our study may also be useful for a better understanding of the physiology of other neuronal GPCRs.

### AUTHOR CONTRIBUTIONS

Delphine Ladarre and Zsolt Lenkei designed the experiments, Delphine Ladarre, Alexandre B. Roland, Stefan Biedzinski and Ana Ricobaraza performed the experiments, Delphine Ladarre, and Stefan Biedzinski analyzed the data and Delphine Ladarre and Zsolt Lenkei wrote the paper.

### ACKNOWLEDGMENTS

This work was supported by a grant from the ANR (L' Agence Nationale de la Recherche) to Zsolt Lenkei (ANR-09-MNPS-004-01). Ana Ricobaraza was supported by a postdoctoral fellowship from the Basque Country Government. We thank Dr. Christophe Leterrier (Marseille) for discussions and advice and Maureen McFadden for the help with the English syntax.

### SUPPLEMENTARY MATERIAL

The Supplementary Material for this article can be found online at: <http://www.frontiersin.org/journal/10.3389/fncel.2014.00426/abstract>

### REFERENCES

- Alger, B. E., and Kim, J. (2011). Supply and demand for endocannabinoids. *Trends Neurosci.* 34, 304–315. doi: 10.1016/j.tins.2011.03.003
- Bacci, A., Huguenard, J. R., and Prince, D. A. (2004). Long-lasting self-inhibition of neocortical interneurons mediated by endocannabinoids. *Nature* 431, 312–316. doi: 10.1038/nature02913

- Bisogno, T., Howell, F., Williams, G., Minassi, A., Cascio, M. G., Ligresti, A., et al. (2003). Cloning of the first sn1-DAG lipases points to the spatial and temporal regulation of endocannabinoid signaling in the brain. *J. Cell Biol.* 163, 463–468. doi: 10.1083/jcb.200305129
- Bodor, A. L., Katona, I., Nyiri, G., Mackie, K., Ledent, C., Hajos, N., et al. (2005). Endocannabinoid signaling in rat somatosensory cortex: laminar differences and involvement of specific interneuron types. *J. Neurosci.* 25, 6845–6856. doi: 10.1523/JNEUROSCI.0442-05.2005
- Castro, L. R., Gervasi, N., Guiot, E., Cavellini, L., Nikolaev, V. O., Paupardin-Tritsch, D., et al. (2010). Type 4 phosphodiesterase plays different integrating roles in different cellular domains in pyramidal cortical neurons. *J. Neurosci.* 30, 6143–6151. doi: 10.1523/JNEUROSCI.5851-09.2010
- Coutts, A. A., Anavi-Goffer, S., Ross, R. A., MacEwan, D. J., Mackie, K., Pertwee, R. G., et al. (2001). Agonist-induced internalization and trafficking of cannabinoid CB1 receptors in hippocampal neurons. *J. Neurosci.* 21, 2425–2433.
- D'Antona, A. M., Ahn, K. H., and Kendall, D. A. (2006). Mutations of CB1 T210 produce active and inactive receptor forms: correlations with ligand affinity, receptor stability, and cellular localization. *Biochemistry* 45, 5606–5617. doi: 10.1021/bi060067k
- Depry, C., Allen, M. D., and Zhang, J. (2011). Visualization of PKA activity in plasma membrane microdomains. *Mol. Biosyst.* 7, 52–58. doi: 10.1039/c0mb00079e
- Freund, T. F., Katona, I., and Piomelli, D. (2003). Role of endogenous cannabinoids in synaptic signaling. *Physiol. Rev.* 83, 1017–1066. doi: 10.1152/physrev.00004.2003
- Gervasi, N., Hepp, R., Tricoire, L., Zhang, J., Lambalez, B., Paupardin-Tritsch, D., et al. (2007). Dynamics of PKA signaling at the membrane, in the cytosol, and in the nucleus of neurons in mouse brain slices. *J. Neurosci.* 27, 2744–2750. doi: 10.1523/JNEUROSCI.5352-06.2007
- Hillard, C. J., Muthian, S., and Kearn, C. S. (1999). Effects of CB(1) cannabinoid receptor activation on cerebellar granule cell nitric oxide synthase activity. *FEBS Lett.* 459, 277–281. doi: 10.1016/S0014-5793(99)01253-3
- Horton, A. C., and Ehlers, M. D. (2003). Neuronal polarity and trafficking. *Neuron* 40, 277–295. doi: 10.1016/S0896-6273(03)00629-9
- Howlett, A. C. (2005). Cannabinoid receptor signaling. *Handb. Exp. Pharmacol.* 168, 53–79. doi: 10.1007/3-540-26573-2\_2
- Howlett, A. C., Reggio, P. H., Childers, S. R., Hampson, R. E., Ulloa, N. M., and Deutsch, D. G. (2011). Endocannabinoid tone versus constitutive activity of cannabinoid receptors. *Br. J. Pharmacol.* 163, 1329–1343. doi: 10.1111/j.1476-5381.2011.01364.x
- Hurst, D. P., Schmeisser, M., and Reggio, P. H. (2013). Endogenous lipid activated G protein-coupled receptors: emerging structural features from crystallography and molecular dynamics simulations. *Chem. Phys. Lipids* 169, 46–56. doi: 10.1016/j.chemphyslip.2013.01.009
- Kano, M., Ohno-Shosaku, T., Hashimoto-dani, Y., Uchigashima, M., and Watanabe, M. (2009). Endocannabinoid-mediated control of synaptic transmission. *Physiol. Rev.* 89, 309–380. doi: 10.1152/physrev.00019.2008
- Kapur, A., Hurst, D. P., Fleischer, D., Whitnell, R., Thakur, G. A., Makriyannis, A., et al. (2007). Mutation studies of Ser7.39 and Ser2.60 in the human CB1 cannabinoid receptor: evidence for a serine-induced bend in CB1 transmembrane helix 7. *Mol. Pharmacol.* 71, 1512–1524. doi: 10.1124/mol.107.034645
- Katona, I., Rancz, E. A., Acsady, L., Ledent, C., Mackie, K., Hajos, N., et al. (2001). Distribution of CB1 cannabinoid receptors in the amygdala and their role in the control of GABAergic transmission. *J. Neurosci.* 21, 9506–9518.
- Katona, I., Sperlagh, B., Sik, A., Kafalvi, A., Vizi, E. S., Mackie, K., et al. (1999). Presynaptically located CB1 cannabinoid receptors regulate GABA release from axon terminals of specific hippocampal interneurons. *J. Neurosci.* 19, 4544–4558.
- Katona, I., Urban, G. M., Wallace, M., Ledent, C., Jung, K. M., Piomelli, D., et al. (2006). Molecular composition of the endocannabinoid system at glutamatergic synapses. *J. Neurosci.* 26, 5628–5637. doi: 10.1523/JNEUROSCI.0309-06.2006
- Kenakin, T. (2004). Principles: receptor theory in pharmacology. *Trends Pharmacol. Sci.* 25, 186–192. doi: 10.1016/j.tips.2004.02.012
- Klarenbeek, J. B., Goedhart, J., Hink, M. A., Gadella, T. W., and Jalink, K. (2011). A mTurquoise-based cAMP sensor for both FLIM and ratiometric read-out has improved dynamic range. *PLoS ONE* 6:e19170. doi: 10.1371/journal.pone.0019170
- Leterrier, C., Laine, J., Darmon, M., Boudin, H., Rossier, J., and Lenkei, Z. (2006). Constitutive activation drives compartment-selective endocytosis and axonal targeting of type 1 cannabinoid receptors. *J. Neurosci.* 26, 3141–3153. doi: 10.1523/JNEUROSCI.5437-05.2006
- Lujan, R., Maylie, J., and Adelman, J. P. (2009). New sites of action for GIRK and SK channels. *Nat. Rev. Neurosci.* 10, 475–480. doi: 10.1038/nrn2668
- Marinelli, S., Pacioni, S., Bisogno, T., Di Marzo, V., Prince, D. A., Huguenard, J. R., et al. (2008). The endocannabinoid 2-arachidonoylglycerol is responsible for the slow self-inhibition in neocortical interneurons. *J. Neurosci.* 28, 13532–13541. doi: 10.1523/JNEUROSCI.0847-08.2008
- Marinelli, S., Pacioni, S., Cannich, A., Marsicano, G., and Bacci, A. (2009). Self-modulation of neocortical pyramidal neurons by endocannabinoids. *Nat. Neurosci.* 12, 1488–1490. doi: 10.1038/nn.2430
- McAllister, S. D., Rizvi, G., Anavi-Goffer, S., Hurst, D. P., Barnett-Norris, J., Lynch, D. L., et al. (2003). An aromatic microdomain at the cannabinoid CB(1) receptor constitutes an agonist/inverse agonist binding region. *J. Med. Chem.* 46, 5139–5152. doi: 10.1021/jm0302647
- McDonald, N. A., Henstridge, C. M., Connolly, C. N., and Irving, A. J. (2007). An essential role for constitutive endocytosis, but not activity, in the axonal targeting of the CB1 cannabinoid receptor. *Mol. Pharmacol.* 71, 976–984. doi: 10.1124/mol.106.029348
- Neves, S. R., Tsokas, P., Sarkar, A., Grace, E. A., Rangamani, P., Taubenfeld, S. M., et al. (2008). Cell shape and negative links in regulatory motifs together control spatial information flow in signaling networks. *Cell* 133, 666–680. doi: 10.1016/j.cell.2008.04.025
- Nomura, D. K., Morrison, B. E., Blankman, J. L., Long, J. Z., Kinsey, S. G., Marcondes, M. C., et al. (2011). Endocannabinoid hydrolysis generates brain prostaglandins that promote neuroinflammation. *Science* 334, 809–813. doi: 10.1126/science.1209200
- Pan, X., Ikeda, S. R., and Lewis, D. L. (1998). SR 141716A acts as an inverse agonist to increase neuronal voltage-dependent Ca<sup>2+</sup> currents by reversal of tonic CB1 cannabinoid receptor activity. *Mol. Pharmacol.* 54, 1064–1072.
- Pertwee, R. G. (2005). Inverse agonism and neutral antagonism at cannabinoid CB1 receptors. *Life Sci.* 76, 1307–1324. doi: 10.1016/j.lfs.2004.10.025
- Phillips, R., Ursell, T., Wiggins, P., and Sens, P. (2009). Emerging roles for lipids in shaping membrane-protein function. *Nature* 459, 379–385. doi: 10.1038/nature08147
- Simon, A. C., Loverdo, C., Gaffuri, A. L., Urbanski, M., Ladarre, D., Carrel, D., et al. (2013). Activation-dependent plasticity of polarized GPCR distribution on the neuronal surface. *J. Mol. Cell Biol.* 5, 250–265. doi: 10.1093/jmcb/mjt014
- Thibault, K., Carrel, D., Bonnard, D., Gallatz, K., Simon, A., Biard, M., et al. (2013). Activation-dependent subcellular distribution patterns of CB1 cannabinoid receptors in the rat forebrain. *Cereb. Cortex* 23, 2581–2591. doi: 10.1093/cercor/bhs240
- Turu, G., Simon, A., Gyombolai, P., Szidonya, L., Bagdy, G., Lenkei, Z., et al. (2007). The role of diacylglycerol lipase in constitutive and angiotensin AT1 receptor-stimulated cannabinoid CB1 receptor activity. *J. Biol. Chem.* 282, 7753–7757. doi: 10.1074/jbc.C600318200
- Uchigashima, M., Narushima, M., Fukaya, M., Katona, I., Kano, M., and Watanabe, M. (2007). Subcellular arrangement of molecules for 2-arachidonoylglycerol-mediated retrograde signaling and its physiological contribution to synaptic modulation in the striatum. *J. Neurosci.* 27, 3663–3676. doi: 10.1523/JNEUROSCI.0448-07.2007
- Yoshida, T., Fukaya, M., Uchigashima, M., Miura, E., Kamiya, H., Kano, M., et al. (2006). Localization of diacylglycerol lipase- $\alpha$  around postsynaptic spine suggests close proximity between production site of an endocannabinoid, 2-arachidonoyl-glycerol, and presynaptic cannabinoid CB1 receptor. *J. Neurosci.* 26, 4740–4751. doi: 10.1523/JNEUROSCI.0054-06.2006

Yoshida, T., Uchigashima, M., Yamasaki, M., Katona, I., Yamazaki, M., Sakimura, K., et al. (2011). Unique inhibitory synapse with particularly rich endocannabinoid signaling machinery on pyramidal neurons in basal amygdaloid nucleus. *Proc. Natl. Acad. Sci. U.S.A.* 108, 3059–3064. doi: 10.1073/pnas.1012875108

**Conflict of Interest Statement:** The authors declare that the research was conducted in the absence of any commercial or financial relationships that could be construed as a potential conflict of interest.

Received: 13 August 2014; accepted: 26 November 2014; published online: 06 January 2015.

*Citation:* Ladarre D, Roland AB, Biedzinski S, Ricobaraza A and Lenkei Z (2015) Polarized cellular patterns of endocannabinoid production and detection shape cannabinoid signaling in neurons. *Front. Cell. Neurosci.* 8:426. doi: 10.3389/fncel.2014.00426

This article was submitted to the journal *Frontiers in Cellular Neuroscience*.

Copyright © 2015 Ladarre, Roland, Biedzinski, Ricobaraza and Lenkei. This is an open-access article distributed under the terms of the Creative Commons Attribution License (CC BY). The use, distribution or reproduction in other forums is permitted, provided the original author(s) or licensor are credited and that the original publication in this journal is cited, in accordance with accepted academic practice. No use, distribution or reproduction is permitted which does not comply with these terms.